Economic Geology, v. 82, pp. 523-545

ECONOMIC GEOLOGY

AND THE

BULLETIN OF THE SOCIETY OF ECONOMIC GEOLOGISTS

VOL. 82 MAY, 1987 NO. 3

Skarn Zonation and Fluid Evolution in the Groundhog Mine, Central Mining District, New Mexico

LAWRENCE D. MEINERT

Geology Department, Washington State University, Pullman Washington 99164-2812

Abstract

The Groundhog mine contains one of the largest and best exposed Zn-Pb-Cu-Ag skarn deposits in the United States. Skarn is formed in Carboniferous limestones spatially associated with a nearly vertical swarm of Early Tertiary granodiorite porphyry dikes. Metal ratios, mineralogy, composition, and fluid inclusion characteristics of the skarn are systematically zoned from northeast to southwest along the >3-km strike length of the system and relative to the original dike-limestone contact. Zn/Cu, Zn/Ag, Pb/Cu, Pb/Zn, and Pb/Ag ratios all increase toward the distal southwest end of the mine where highest Zn, Pb, and total metal grades also occur.

Endoskarn is zoned in terms of the relative proportions and manganese content of epidote and chlorite. In the Northeast zone, skarn is zoned away from dikes in the sequence: garnet to pyroxene to pyroxenoid to marble. In the Central skarn zone, garnet is absent and pyroxene begins the zonation sequence at the dike contact. In the Southwest zone, pyroxene is less abundant and pyroxenoid locally begins the zonation sequence. Sphalerite-galena-pyrite-quartz-carbonate are present in all skarn zones and in carbonate replacement mantos and chimneys beyond skarn. Distal mineralogical zones (e.g., pyroxenoid and manto) are more extensive to the southwest. In general, the skarn zonation sequence is wider and more fully developed in pure, coarse-grained limestone than in silty, carbonaceous, or fine-grained limestone. High permeability and water/rock ratio are considered the dominant controls on skarn size.

Most skarn minerals, including garnet, pyroxene, pyroxenoid, ilvaite, amphibole, chlorite, carbonate, and sphalerite, are enriched in manganese. Pyroxene becomes more manganese rich (up to 85 mole % johannsenite):(1) toward marble, (2) along strike to the southwest, (3) at higher elevations, and (4) in coarser grained, cleaner limestones. The more manganese-rich pyroxenes formed from fluids which are distal in the overall zonation sequence. In contrast, pyroxene formed in proximal locations (dike contact, Northeast skarn zone, low elevation, fine-grained, impure limestone) is enriched in magnesium. Pyroxene-forming fluids are depleted first in Mg, then in Fe, and finally in Mn, as proposed by Burt (1977).

Fluid inclusion homogenization temperatures are lower than for most zinc skarns. In the Northeast skarn zone the average homogenization temperature is 337°C and salt daughter minerals are present in garnet and pyroxene (inclusions without daughter minerals average 8.5 wt % NaCl), whereas salt daughter minerals are absent in the Central and Southwest skarn zones and average homogenization temperatures and salinities are 320°C, 7.3 wt percent NaCl, and 293°C, 6.2 wt percent NaCl, respectively. Pressure estimates from rare clusters of fluid inclusions with evidence for boiling are between 155 and 175 bars.

Skarn thermal gradients calculated from fluid inclusion homogenization temperatures are 35°C from dike to marble front and 50°C from dike to the limit of alteration (carbonate replacement mantos and chimneys). The calculated average thermal gradient along strike ranges from 8°C/km along the dike contact to 23°C/km along the marble front. The calculated thermal gradients and measured pyroxene compositions are in general agreement with published experimental studies of clinopyroxene stability relations.

The variations in skarn metal ratios, mineralogy, composition, and fluid inclusion characteristics have been incorporated into a general model for zinc skarn formation which can be applied to the hierarchy of zinc skarns summarized by Einaudi et al. (1981) and as a guide to exploration. The distal end of this zinc skarn hierarchy is transitional to manto and chimney carbonate replacement deposits which contain few, if any, calc-silicate minerals.

0361-0128/87/662/523-23$2.50

Introduction

THE Groundhog mine contains one of the largest and best exposed zinc skarn deposits in the United States. It also contains numerous carbonate replacement manto and chimney orebodies and base metal veins in overlying volcanic rocks. It is located in the Central mining district (Fig. 1) approximately 25 km east of Silver City, New Mexico, in a region containing a variety of porphyry copper, skarn, and vein deposits. Underground mining in the Groundhog fault zone began prior to 1869 with the recovery of shallow supergene vein ore (Raymond, 1870). Early mining was not on a large scale until ASARCO, Inc., acquired the property in 1928 (Lasky, 1936) and began developing the deeper levels of the mine where significant tonnages of Zn-Pb-Ag skarn and carbonate replacement ore were encountered. The Groundhog mine produced nearly 3 million tons of high-grade ore until the mine was closed in 1980 due to a combination of declining metal prices and increasing smelter costs. Skarn metal content (based upon production) is zoned within the mine (Table 1) and, in general, copper decreases and lead and zinc increase to the southwest along the >3-km strike length of the skarn system. This metal zonation is accompanied by systematic changes in skarn mineralogy and fluid inclusion characteristics, thus providing a unique opportunity to study a large well-exposed zinc skarn deposit and associated carbonate replacement mantos and chimneys.

The ore deposits in the Central mining district have been the subject of more than 100 papers ranging from broad studies of district-wide geology and zonation patterns (Lindgren et al., 1910; Paige, 1916; Spencer and Paige, 1935; Lovering, 1953; Jones et al., 1967; Hernon and Jones, 1968) to detailed investigations of single mines (Paige, 1909; Graton, 1910; Schmitt, 1939; Nielsen, 1968; Ahmad and Rose, 1980; Abramson, 1981) to geochemical studies and comparisons with other districts (Graf and Kerr, 1950; Burnham, 1959; Rose, 1970; Taylor and Fryer, 1983; Parry et al., 1984). The present paper concentrates on the Groundhog mine and a study of fluid evolution involving mineral composition and fluid inclusion variations along the length of the Groundhog skarn system. This study is based on detailed underground mapping (approximately 1:500 and 1:100) of the 2100, 1950, and 1650 mine levels and selective relogging of more than 100 diamond drill holes.

Geology and Ore Deposits

The regional geology and ore deposits of the Central mining district have been described in detail by Hernon et al. (1964), Jones et al. (1967), and Hernon and Jones (1968). On a district scale, there are three distinct styles of mineralization: (1) porphyry copper

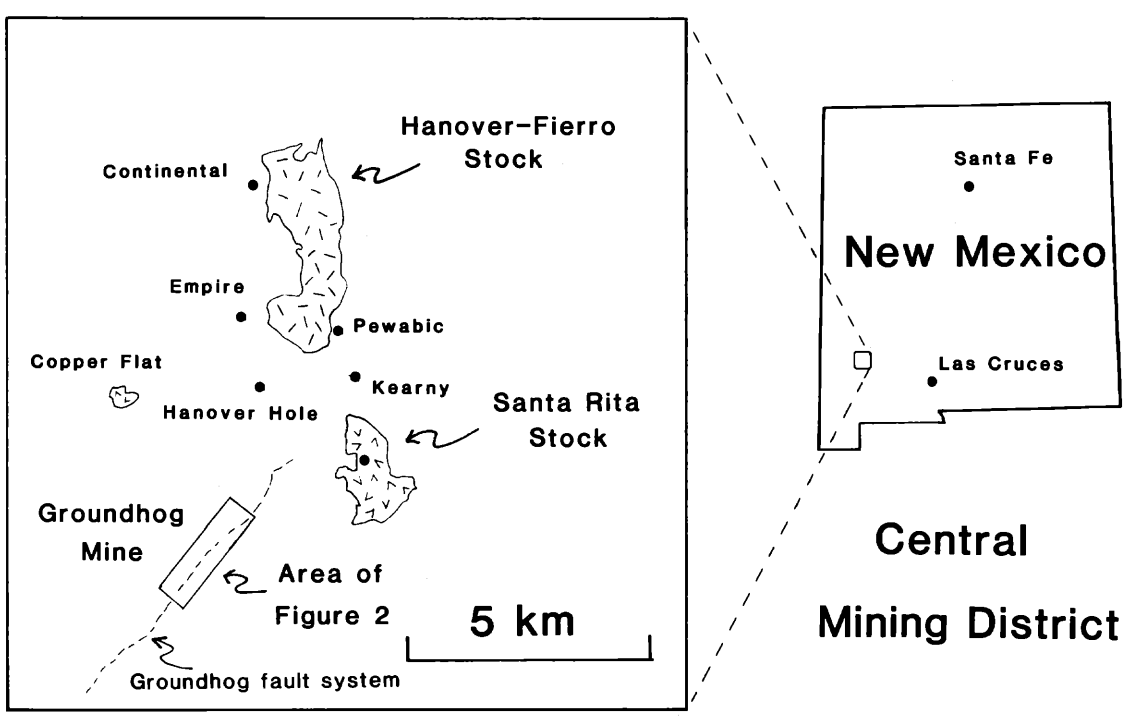

FIG. 1. Location map for the Groundhog mine and other localities in the Central mining district, New Mexico.

TABLE 1. Skarn Grade, Tonnage, and Metal Ratios from the Groundhog Mine

Mine area	Lucky Bill	Groundhog-San Jose	Ivanhoe
Location	Southwest zone	Central zone	Northeast zone
Tonnage (P + R)	84,408	1,867,106	486,403
Grades			
% Cu	0.47	0.61	0.64
% Pb	6.69	2.94	1.60
% Zn	14.17	13.66	12.60
oz/ton Ag	0.89	1.60	0.98
Metal ratios			
Zn/Pb	2.1	4.7	7.9
Zn/Cu	30.2	22.4	19.7
Zn/Ag	15.9	8.5	12.9
Pb/Ag	7.5	1.8	1.6
Pb/Cu	14.2	4.8	2.5
Ag/Cu	1.9	2.6	1.5

Total Groundhog mine production to September 1977: 2,987,340 tons averaging 12.3% Zn, 3.6% Pb, 1.3% Cu, and 2.5 oz/ton Ag (data from Lasky, 1936; Lasky and Hoagland, 1950; and T. Dalla Vista, pers. commun., 1980)

Abbreviations: P = production, R = reserves

deposits with related copper skarn occur at Continental (Einaudi, 1982), Copper Flat (Hernon and Jones, 1968), and Santa Rita (Nielson, 1968; Amad and Rose, 1980; Reynolds and Beane, 1985); (2) iron and zinc skarn deposits occur in a broad zone around the Hanover-Fierro pluton, including the Pewabic (Schmitt, 1939), Empire, Kearney, and Oswaldo mines (Hernon and Jones, 1968), and also along several north- and northeast-trending dike swarms, including the Groundhog and Grant County mines; and (3) lead-zinc-silver veins and replacements occur at the Bullfrog, Georgetown, upper Groundhog, Slate, and Three Brothers mines (Lasky, 1942; Hernon and Jones, 1968).

Most workers consider the ore deposits in the Central mining district to be the result of a single prolonged mineralization event related to a complex series of granitic stocks and dikes (Hernon and Jones, 1968). Based upon field relations, Jones et al. (1967) distinguished three magmatic events within the Central mining district: early sills, plutons of granodiorite and quartz monzonite, and dike swarms of granodiorite and quartz monzonite porphyry. However, the contemporaneity of the discordant igneous rocks is questionable in that K-Ar dating by McDowell (1971) suggests that the Hanover-Fierro pluton may be 10 m.y. older than the Santa Rita stock. Furthermore, the differences in style of skarn mineralization associated with the two stocks led Einaudi (1982) to conclude that the zinc skarns and copper skarns in the Central mining district are not related. The Groundhog skarn is mineralogically similar to the zinc skarns surrounding the Hanover-Fierro pluton and is part of a district Zn/Pb zonation trend (up to 140:1 near the pluton, 50:1 at Hanover, 8:1 at the northeast part of the Groundhog mine, and 2:1 at the distal southwest part of the mine; Hernon and Jones, 1968, and Table 1, this study) which is centered on the Hanover-Fierro pluton and not the Santa Rita or Copper Flat stocks.

Skarn ore in the Groundhog mine occurs in Paleozoic sedimentary rocks adjacent to a northeast-trending, nearly vertical dike swarm which is subparallel to the Groundhog fault system (Fig. 2). Most skarn is restricted to two units, the Pennsylvanian Oswaldo Formation and the Mississippian Lake Valley Formation. Within the mine the Oswaldo Formation is broken down informally into the Upper Blue limestone, the Middle Blue limestone, and the parting shale. The underlying Lake Valley Formation is informally subdivided into the Hanover limestone and the Lower Blue limestone. The Hanover limestone is a very pure white, coarse-grained (0.2–2 mm) crinoidal limestone, whereas the Upper, Middle, and Lower Blue limestones are fine-grained (<0.01–0.2 mm), black, carbonaceous, silty, slightly argillaceous limestones. The magnesium (and presumably iron and manganese) content of the Hanover, Upper, Middle, and Lower Blue limestones does not vary significantly, being respectively: 0.19, 0.14, 0.10, and 0.44 wt percent MgO (Schmitt, 1939). Although skarn has formed in all of these units, the bulk of the economic skarn and carbonate replacement mineralization in the Groundhog mine occurs in the Hanover limestone. This may in part be due to the 3- to 10-m-thick parting shale which overlies the Hanover limestone and which may have served to dam mineralizing fluids in the underlying beds.

Because the sedimentary layers in the Groundhog mine are almost horizontal, with an average dip of 3° to the southwest, none of the deeper sedimentary units which crop out elsewhere in the district are exposed in the mine. A few deep exploratory drill holes have encountered small amounts of copper and zinc mineralized skarn in the underlying Silurian Fusselman Dolomite and the Ordovician Montoya and El Paso Dolomites, but these units are not present in the mine workings. Because the mine workings largely follow the Hanover limestone, approximately the same stratigraphic section is exposed in all the parts of the mine. This is important because in the present study, skarn samples from three different parts of the mine, the Northeast, Central, and Southwest zones, are compared.

There are two distinct dike types in the Groundhog mine, both of which are considered to be Tertiary in age (Jones et al., 1967). The granodiorite porphyry dikes (Table 2) are spatially associated with skarn. These dikes range in width from 1 to 50 m and are strongly altered to epidote-rich endoskarn near limestone contacts. There is little correlation between dike

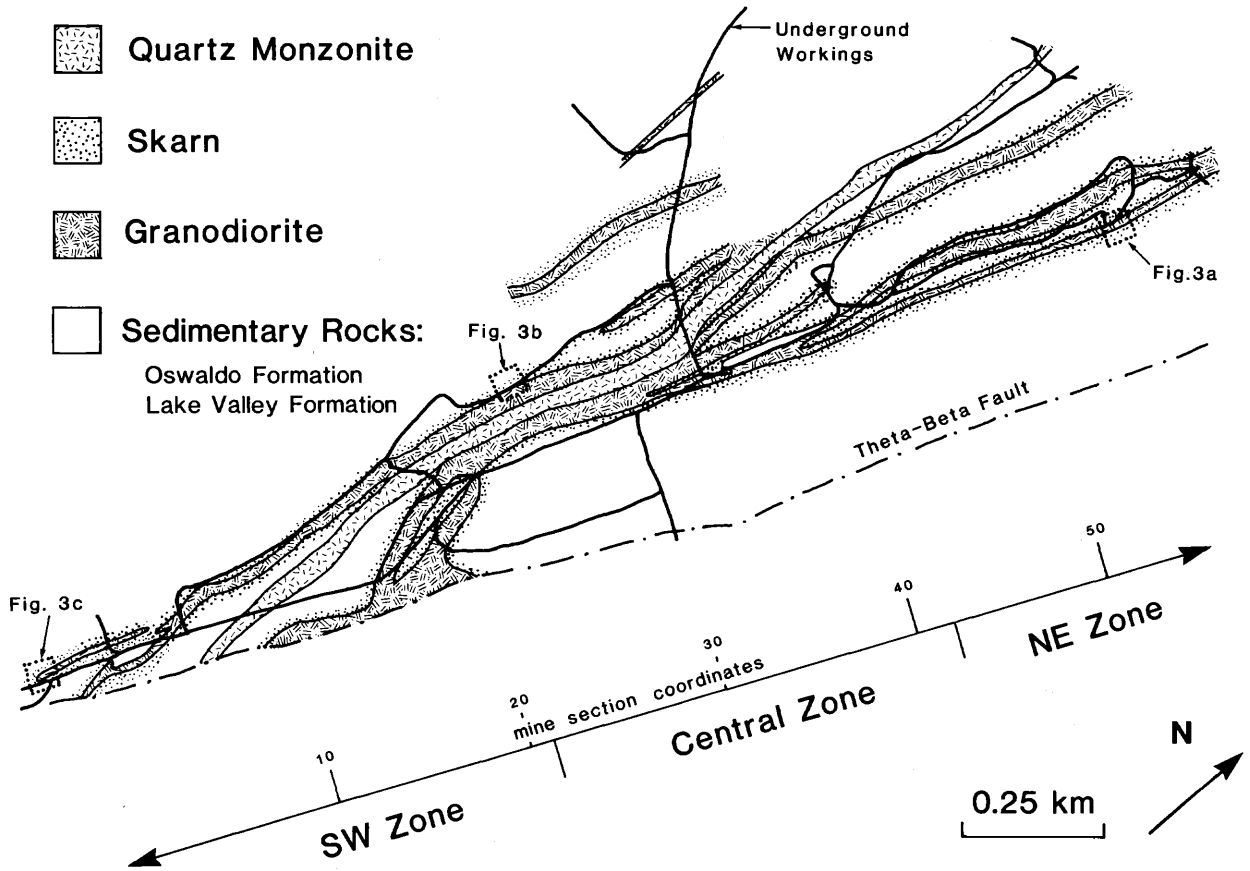

FIG. 2. Composite geologic map of the Groundhog mine, based on underground mapping from the 1950 and 1650 levels (ASARCO, unpublished company maps and the present study).

TABLE 2. Representative Dike Compositions from the Groundhog Mine

Dike type	Granodiorite porphyry		Quartz monzonite porphyry	
Sample no.	GH-22	1[1]	GH-X'	1[2]
SiO_2	64.60	64.63	67.38	66.16
Al_2O_3	16.08	15.68	16.21	15.70
Fe_2O_3	2.10	2.75	1.53	1.30
FeO	2.41	1.96	1.75	1.62
MgO	1.98	1.00	1.42	1.20
CaO	5.41	4.16	3.54	3.66
Na_2O	1.61	2.10	3.83	3.46
K_2O	4.90	2.73	3.56	3.58
TiO_2	0.53	0.60	0.40	0.37
P_2O_5	0.24	0.31	0.19	0.21
MnO	0.34	0.20	0.18	0.17
Total	100.00[3]	96.12	100.00[3]	97.43

[1] Groundhog mine, Vanadium area; L. Entwistle, analyst (Schmitt, 1954)

[2] Groundhog mine, 1634 drift; L. D. Trumbull, analyst (Jones et al., 1967)

[3] Analyses by X-ray fluorescence, Department of Geology, Washington State University (Meinert, 1983); analyses are normalized on a volatile-free basis with the oxidation state of iron set at the arbitrary ratio of $Fe_2O_3/FeO = 0.87$

size and the extent or intensity of skarn-endoskarn alteration. However, the amount of skarn and number of dikes is greater toward the northeast part of the system. As will be discussed in a later section, the skarn mineralogical zoning also indicates that the northeast and deeper parts of the skarn system were more proximal to the fluid source than were the southwest and shallower parts of the system. Skarn-forming fluids were probably contemporaneous with or slightly later than the granodiorite dikes and are assumed to be related to the same magmatic source. Variations in skarn mineralogy and metal content suggest that the magmatic source lies at depth to the northeast, although it is not clear that it is connected to either the Santa Rita or Hanover-Fierro plutons. On a district scale, Jones et al. (1967) distinguished three different generations of granodiorite dikes, all of which are considered to be part of an early Tertiary igneous event.

The quartz monzonite porphyry dikes (Table 2) in the Groundhog mine do not have any skarn associated with them and generally lack significant endoskarn alteration. These dikes have chilled contacts against both limestone and the granodiorite porphyry dikes

and therefore are younger. The quartz monzonite dikes do not appear to have introduced or circulated large volumes of fluid. They are considered to postdate mineralization on both a mine and regional scale (Hernon and Jones, 1968).

Although numerous small normal faults produce minor offsets in veins and dikes, the only major faults are the Copper Glance fault and those of the Groundhog fault system, which consists of the Theta, Beta, and Gamma faults. The Theta fault has about 80 m and the Beta fault has about 325 m of postmineralization offset (unpublished ASARCO reports, maps, and cross sections). Total offset on the Theta-Beta fault system (Fig. 2) is estimated at about 600 m, southeast side down. Both skarn and dikes are truncated by these faults. Fault gouge in the Theta-Beta fault contains abundant chlorite and pyrite. However, no skarn or other alteration of limestone has been observed at the fault contact, indicating that the present exposure of the Theta-Beta fault was not a major conduit for skarn-forming fluids.

Hydrothermal Alteration and Skarn Formation

Endoskarn

Both granodiorite and quartz monzonite porphyry dikes are altered near carbonate contacts. The quartz monzonite porphyry dikes typically contain 1 to 2 percent disseminated pyrite and a very minor sericite dusting of plagioclase phenocrysts, but alteration near carbonate contacts is limited to a gradual increase of chlorite (and minor epidote) in the rock matrix which makes the rock look darker in hand specimen. This altered zone is commonly less than 1 cm but may be up to 1 m in thickness.

In contrast, the granodiorite porphyry dikes typically contain up to 5 percent disseminated pyrite and have a well-developed zoned endoskarn near carbonate contacts. Endoskarn consists of pink (in hand specimen) epidote replacing feldspar and hornblende phenocrysts and a mixture of chlorite, green epidote, quartz, and calcite replacing both mafic minerals and groundmass feldspar. In general, the pink epidote is more manganese rich and more distal to endoskarn vein centers than is the green epidote (Table 3). Large fracture-controlled endoskarn veins are common with quartz-calcite cores, thin epidote selvages, and a diffuse halo of epidote-chlorite replacing mafic minerals and some feldspar in the wall rock.

Exoskarn

On the scale of the entire mine (Fig. 2), skarn occurs as a relatively thin mantle adjacent to granodiorite porphyry dikes. However, there is a large variation in skarn thickness and geometry on a local scale (Fig. 3). Some of the causes of variation in skarn thickness are the permeability, grain size, and composition of the protolith. Skarn formed from the coarse-grained Hanover limestone is typically 5 m or more in thickness whereas a similar complete skarn zonation pattern in the fine-grained carbonaceous Blue Limestones is typically less than 5 m thick and may be only a few centimeters. In general, skarn in the proximal northeast part of the system is conformable to dike contacts. Farther to the southwest, in the more distal part of the system, there are pods and lenses of skarn which extend away from the dike contacts along bedding and structural pathways; locally, skarn is absent at the dike content (Fig. 4C). Skarn is typically zoned away from the dikes and along the 3-km strike length of the dike swarm. Figure 4 illustrates typical skarn geometries and zonation patterns in the Southwest, Central, and Northeast skarn zones.

Skarn in the northeast part of the system typically consists of three zones: the marble front, massive pyroxene skarn, and the dike contact. At the marble front, skarn is always separated from limestone by a zone of recrystallized and bleached calcite with minor quartz. Individual calcite grains may be up to one or two centimeters in diameter and usually are elongate

TABLE 3. Representative Endoskarn Epidote and Chlorite Analyses (in wt %)

Sample no.	T4-1-1137-8	1558-111	T4-1-1137-5	1423-12
Mineral	Epidote	Epidote	Chlorite	Chlorite
Color	Pink	Green	Green-black	Green-black
SiO_2	36.56	36.92	24.51	23.68
Al_2O_3	22.66	23.22	19.05	19.14
Fe_2O_3/FeO	13.41	13.03	26.77	35.11
MgO	0.66	0.05	9.50	5.34
MnO	2.89	0.31	7.22	3.98
CaO	21.01	24.21	<0.01	<0.01
K_2O	<0.01	<0.01	<0.01	<0.01
Na_2O	0.01	<0.01	<0.01	<0.01
TiO_2	0.32	0.01	0.03	<0.01
Total	97.52	97.74	87.08	87.25

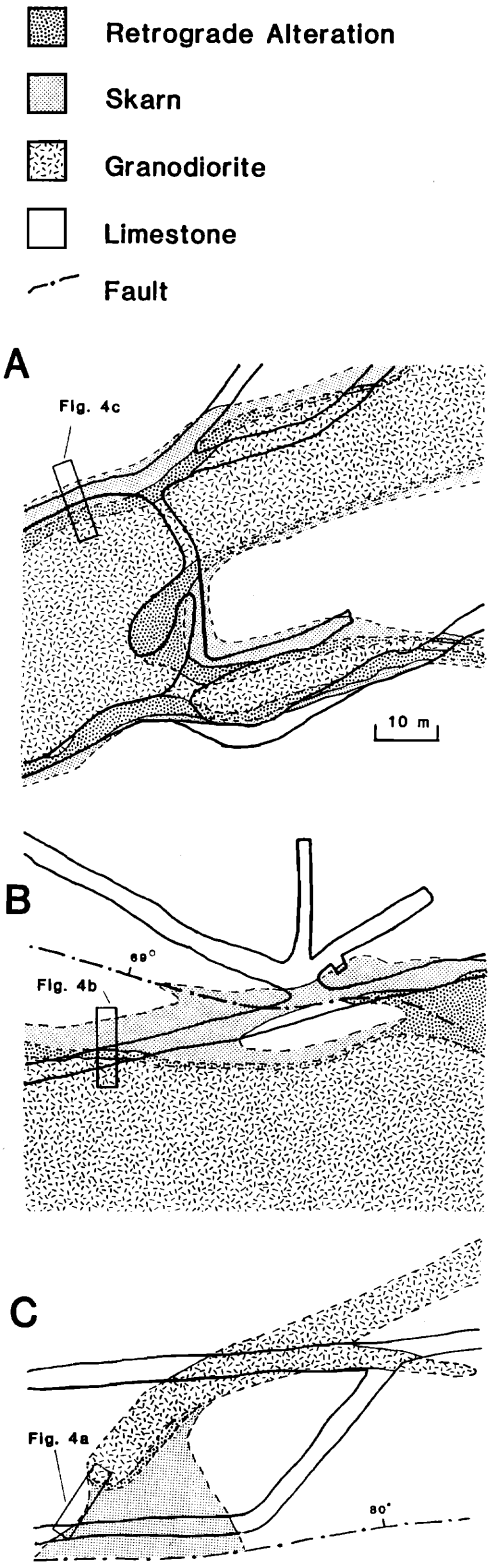

FIG. 3. Typical geometry of skarn, granodiorite porphyry dikes, and chlorite-pyrite retrograde alteration based upon underground workings (dark lines outline drifts) and drill core intercepts. A. Northeast skarn zone, 1638-8 drift. B. Central skarn zone, 1910 drift. C. Southwest skarn zone, 1902 drift.

parallel to the skarn contact. Some calcite grains have bent twin lamallae and cataclastic borders indicating that this zone has been a locus for shearing after skarn was formed due to the mechanical contrast between relatively brittle skarn and ductile limestone. The bleached zone generally mantles skarn but also extends outward into unaltered limestone along fractures and bedding planes. Locally sphalerite, pyrite, and minor galena occur disseminated (<1% by volume) in bleached marble or in relict carbonate patches within skarn. Minor amounts of manganese-rich pyroxenoid crystals (mostly rhodonite; microprobe compositions are discussed in a later section) occur in some relict carbonate patches within skarn and between bleached limestone and massive skarn.

Massive skarn consists of coarse-grained, euhedral pyroxene crystals (with interstitial sphalerite and minor pyrite, magnetite, and/or hematite) oriented perpendicular to the marble front in multiple metasomatic bands separated by turbid zones with a felted texture (Fig. 5A). Individual pyroxene crystals terminate as pyroxene fibers or crystallites growing into quartz and carbonate at the marble front (Fig. 5B). The turbid, felted zones are interpreted as crystallites of previous skarn fronts which were bypassed and then overgrown by later skarn-forming fluids. Thus, skarn is produced by metasomatic fluids which infiltrate through previously formed skarn and then form veins and irregular metasomatic fronts in limestone. As metasomatic veins and fronts coalesce, patches of limestone are segregated and recrystallized as calcite patches surrounded by coarse-grained skarn. These relict calcite patches can then be replaced by subsequent skarn-forming fluids. A consequence of this skarn growth model is that each successive pulse of fluid is buffered by previously formed skarn prior to reacting with carbonate either at the marble front or in relict limestone patches.

The dike contact is the main locus of fluid movement. Both massive pyroxene-sphalerite exoskarn and epidote-chlorite endoskarn are formed adjacent and parallel to the dike contact. This contact zone also contains garnet-chalcopyrite veins and is the focus of superimposed chlorite-sulfide retrograde alteration. Garnet veins in the Groundhog mine are restricted to the Northeast skarn zone. Garnet occurs as layers and veins which cut the massive pyroxene-sphalerite skarn near the dike contact. Some of the garnet is associated with chalcopyrite and locally this garnet-rich skarn assays 2 to 3 percent Cu. Pyrite and magnetite are particularly abundant in these chalcopyrite-rich areas.

Hydrous minerals such as chlorite and amphibole, which are normally thought of as retrograde skarn minerals (Einaudi et al., 1981), have a very specific spatial occurrence in the Groundhog mine. In almost every skarn occurrence, a zone of massive chlorite-pyrite separates endoskarn from exoskarn. This zone

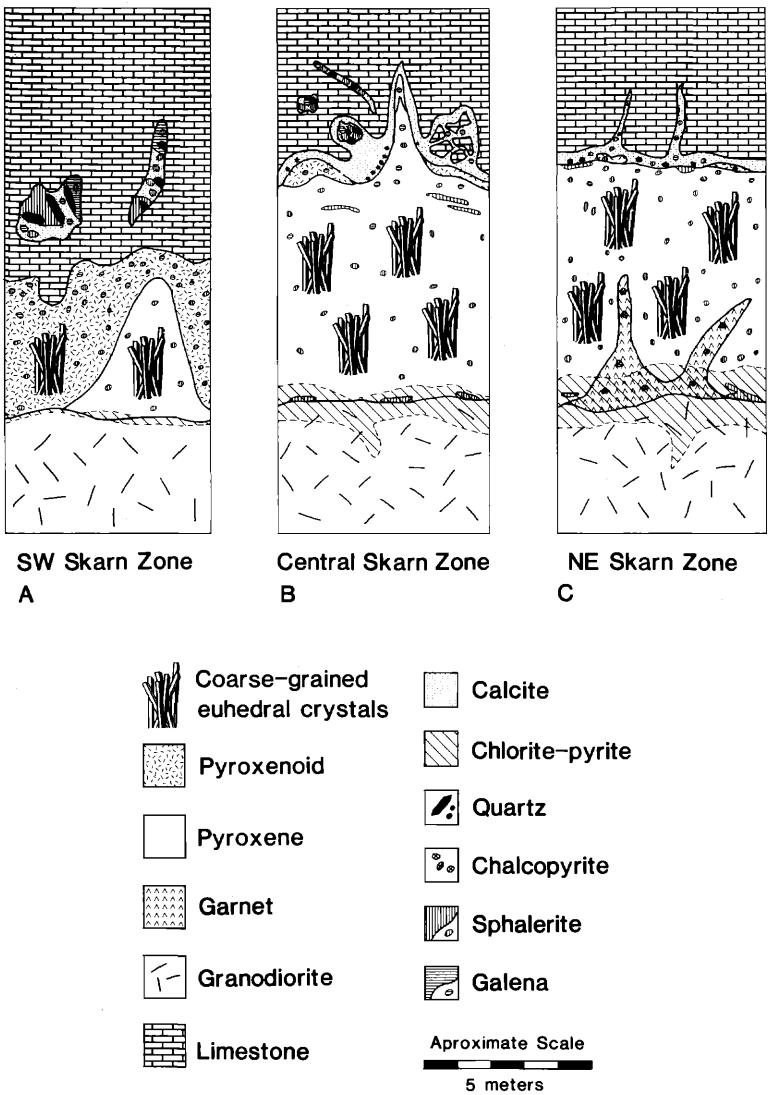

FIG. 4. Idealized skarn mineralogy and zonation patterns from (A) the Southwest skarn zone, (B) the Central skarn zone, and (C) the Northeast skarn zone.

can be quite high grade, contain up to 50 percent sulfides (mostly pyrite), and can be <1 cm to 5 m in width. Other minerals which occur in this zone include amphibole, ilvaite, quartz, calcite, clay, hematite, sphalerite, tetrahedrite, galena, and chalcopyrite. Catlin (1981, 1984) also described the occurrence of tiny blebs of cubanite in chalcopyrite and polybasite in galena. In some samples these minerals have partly to completely replaced skarn or endoskarn minerals and pseudomorphs are easily recognizable. However, in most samples the chlorite-pyrite is massive and there is no trace of preexisting calc-silicate minerals. Minor amphibole and chlorite also occur as typical retrograde replacements of pyroxene in skarn away from the dike contact.

With the exception of garnet, which occurs only in the Northeast skarn zone, all the previously described minerals and skarn zones also occur in the Central and Southwest parts of the Groundhog skarn system. The major differences are of mineral abundance, proportions, and grain size. In the Central skarn zone, pyroxenoid is much more abundant than in the Northeast zone and the extent of bleaching, brecciation, and mineralization of limestone beyond the skarn is much greater. Chalcopyrite as a separate mineral phase is less common, although chalcopyrite inclusions within sphalerite grains are perhaps more abundant. Bands of pyroxenoid are centimeters to tens of centimeters thick at some marble front contacts in the Central skarn zone. In places, veins or fronts of limestone bleaching have partially coalesced creating patchy breccia zones. Sulfide-quartz-carbonate

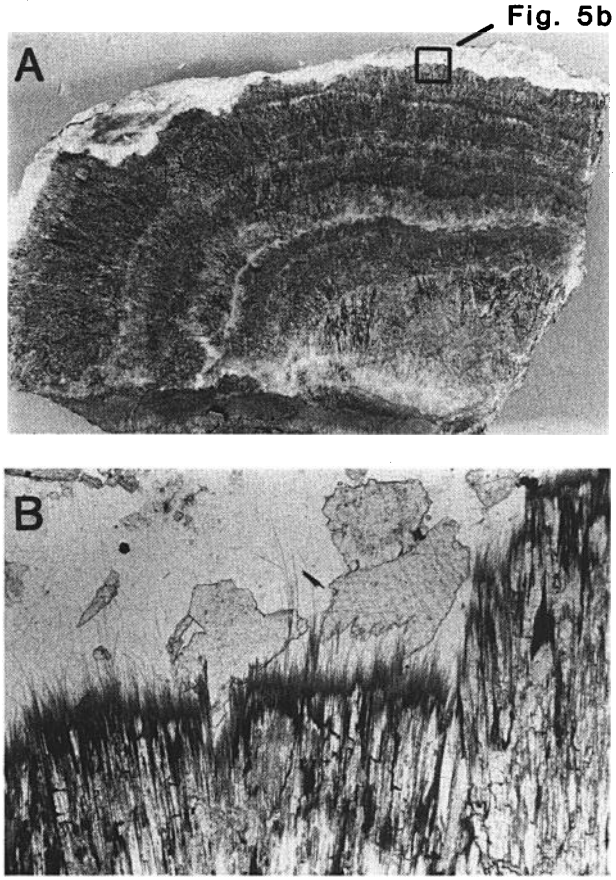

FIG. 5. Skarn development at the marble front (sample GH-17, 1830-8-1 drift). A. Multiple metasomatic pyroxene growth bands parallel to skarn front (specimen is 8 cm wide). B. Photomicrograph of fibrous pyroxene growth into carbonate and quartz at the marble front (width of photo = 2.5 mm, same sample as in A).

± chlorite replacements in the bleached limestone are larger than in the Northeast zone and in some places mineralized veins and replacements extend out into limestone beyond the zone of visible bleaching. These replacements containing quartz, manganese-rich carbonate, pyrite, sphalerite, and local chlorite are of particular interest because they are compositionally similar to skarn yet contain no calc-silicate minerals.

In the Southwest skarn zone both massive pyroxene skarn and retrograde alteration are less common. Manganese-rich pyroxenoid is the dominant calc-silicate mineral in this zone and both pyroxenoid and pyroxene are very coarse grained; individual crystals are typically several centimeters long. Chalcopyrite is present only as inclusions in sphalerite. Perhaps the greatest change toward the southwest in the Groundhog system is that sulfide-quartz-carbonate ± chlorite veins, vugs, and massive replacements of limestone without skarn are quite common. In several places mineralizing fluids apparently were dammed in Hanover Limestone beneath the Parting Shale resulting in massive sulfide mantos. As with the previously described vugs, these mantos contain quartz, manganese-rich carbonate, chlorite, and sulfides but no calc-silicate minerals.

Mineral Composition and Zonation

Most of the skarn minerals are enriched in manganese, a characteristic of this skarn class (Einaudi et al., 1981). The johannsenitic pyroxene is perhaps most diagnostic, but garnet, pyroxenoid, ilvaite, amphibole, chlorite, carbonate, and sphalerite also are enriched locally in manganese. As with the overall skarn mineralogy, this manganese enrichment is zoned within the Groundhog system. In addition to a distinct skarn zonation along strike and a more compressed zonation perpendicular to the granodiorite dikes, there is also a distinct but less regular compositional variation with elevation within the skarn system and as a function of host rock composition. As pointed out by Einaudi and Burt (1982), temperature and f_{O_2} variations can also have a significant effect on skarn mineral compositions.

Each of the four main variables within the Groundhog system: distance along strike, position within skarn, host-rock composition, and elevation, affects the skarn mineralogy and mineral composition of a given sample. The complex interaction of these variables can best be studied in pyroxene which occurs throughout the skarn system and which has major element (Fe, Mg, Mn) solid solution variability. Individual pyroxene crystals from more than 200 samples were analyzed by electron microprobe (Table 4) to document the compositional effect of each of the four main variables. Most individual crystals were compositionally homogeneous; no consistent zonation patterns were recognized within single grains. When all the analyses are plotted together (Fig. 6), they fill a large part of the diopside-hedenbergite-johannsenite field. In particular, the pyroxene compositional gap proposed by Einaudi and Burt (1982) is absent. However, even in this plot it is apparent that there are certain groupings; for example, pyroxene from the marble front is more manganese rich and pyroxene formed in fine-grained carbonaceous limestone is more magnesium rich than most other pyroxenes.

The effect of each of the four variables can be isolated in a series of triangular compositional plots (Fig. 7A-C). For a given location within the Groundhog mine, pyroxene formed near granodiorite dike contacts (proximal to fluid channelways) is magnesium rich (Fig. 7A). Pyroxene in the middle of the skarn is enriched in iron and slightly in manganese, whereas pyroxene at the marble front is very manganese rich but has an Fe/Mg ratio similar to the bulk of skarn pyroxene.

A transect of average pyroxene compositions from dike contact to mid-skarn to marble front in the Southwest zone of the skarn system is more manganese rich than a similar transect in the Northeast zone (Fig. 7A). The effect of a more southwestern, or distal, location within the skarn system is a great enrichment of any given skarn pyroxene position (e.g., dike contact, mid-skarn, or marble front) in manganese and a slight depletion in iron.

The chief contrast in skarn host-rock composition is between the pure, white, coarse-grained, Hanover limestone and the dark gray, fine-grained, silty, carbonaceous Blue limestones. For purposes of comparison, carbonate protoliths were classified as "clean" if they were white in hand specimen and lacked microscopically visible carbonaceous matter. In contrast they were classified as "carbonaceous" if they were dark gray or black in hand specimen or contained significant microscopic carbonaceous matter. For a given location within the skarn system, pyroxene formed in a carbonaceous protolith is finer grained, richer in magnesium, and poorer in manganese than pyroxene formed in clean limestone (Fig. 7B). The effect of location within the overall skarn system is again apparent in Figure 7B in that pyroxene formed from each of the different categories of limestone is enriched in manganese toward the southwest.

To assess the effect of elevation upon pyroxene composition, the analyzed samples were divided into three categories, high (>4,300 ft), middle (4,075–4,300 ft), and low (<4,075 ft), based on their position relative to the mapped mine levels (Fig. 7C). For a given location within the skarn, pyroxene from higher elevations is more manganese rich and pyroxene from lower elevations is more magnesium rich. For a given elevation within the skarn system, pyroxene is enriched in manganese to the southwest. This manganese enrichment in pyroxene along strike and at higher elevations is not likely the result of protolith compositional variations because typical limestone manganese contents are quite low (avg 0.2 wt % MnO, Barber, 1974) relative to skarn minerals which contain up to 42 wt percent MnO (Tables 3–8). Furthermore, the stratigraphically higher Upper and Middle Blue limestones are carbonaceous, whereas the underlying Hanover limestone is clean. Thus, the trend of manganese enrichment with elevation is opposite that which would be expected simply on the basis of stratigraphic-compositional variations.

For an individual sample the absolute effect of skarn location, position in skarn, protolith composition, or elevation, on resultant pyroxene composition is difficult to evaluate because some of these variables may be partly compensatory. However, for the skarn system as a whole a general pattern emerges which has predictive value and exploration significance. Pyroxene in the Groundhog system is compositionally zoned, becoming more manganese rich and less magnesium rich: (1) along strike to the southwest, (2) toward the marble front, and (3) higher in the system. There is also an apparent buffering effect by the protolith in that pyroxene formed from carbonaceous limestone has a higher Mg/Fe ratio and less manganese than pyroxene formed from the pure crinoidal limestone.

Sphalerite is also found throughout the skarn but is not as compositionally variable as pyroxene. The MnS content is typically about 0.5 percent (range 0.1–1.2%) and CdS less than 0.2 percent. However, the FeS content of sphalerite is somewhat higher and, like pyroxene, varies as a function of location and protolith composition. Based on electron microprobe analyses of approximately 100 samples, the FeS content (mole % average and range) of sphalerite in skarn formed from clean, coarse-grained Hanover limestone is 5.0 percent (2.7–6.3%) in the Northeast skarn zone, 4.1 percent (3.0–5.1%) in the Central zone, and 3.5 percent (2.1–4.5%) in the Southwest zone. The FeS content of sphalerite in skarn formed from fine-grained, carbonaceous limestone is 4.8 percent (3.1–7.2%) in the Northeast, 3.1 percent (1.9–4.0%) in the Central, and 2.8 percent (1.7–4.5%) in the Southwest skarn zone. Thus, for a given location in the skarn system, sphalerite in skarn formed from fine-grained, carbonaceous limestone has a lower iron content than that formed from coarser grained, non-carbonaceous limestone.

Sphalerite from the carbonate replacements beyond skarn (i.e., no calc-silicate minerals present) is distinctly different from that in skarn. Sphalerite from replacements is deep red in thin section (skarn sphalerite is pale yellowish-green) and contains significantly more iron; three analyzed samples yielded 11.8, 12.4, and 14.8 mole percent FeS.

Garnet in the Groundhog mine is part of the grandite solid solution series (largely andradite) and is of mineralogical interest in that there is not enough aluminum in most of the garnets to balance the relatively high manganese content. Thus, instead of using the spessartine molecule for stoichiometric calculations, the theoretical calderite end member ($Mn_3Fe_2Si_3O_{12}$, Dunn, 1979) must be used (Table 5).

Pyroxenoid occurs at the marble front and in carbonate-filled vugs (interpreted to be recrystallized relict patches of limestone) in skarn. It is compositionally variable (Table 6, Fig. 8) yet there does not appear to be any correlation between its composition and any of the variables described for pyroxene and sphalerite. In thin section some pyroxenoid crystals have alternating clear and either brown or green lamallae. The optically distinct lamallae contain different amounts of Fe, Mn, and Mg, yet there is little correlation between composition and color or mode of occurrence. On the scale of a 1-μ diameter electron

TABLE 4. Electron Microprobe Analyses of Pyroxene (in wt %)

Sample no.	1902-101b	1286-35	1902-68b	335-32	224-20	335-63	1479-6	1902-7	851-62b	2173-547	T5-2-1650e	1908-13
Section no.[1]	7.2	−3.8	19.5		−2.5	19.4	22.3	39.7	30.3	32.4	21.5	26
Skarn position[2]	D	S	S	S	M	M	D	D	D	S	S	S
Elevation[3]	M	L	M	H	H	H	M	M	H	L	L	M
Protolith[4]	H	C	H	C	H	C	H	C	H	H	C	H
SiO_2	50.71	51.66	49.58	51.43	49.45	50.85	49.86	51.51	48.15	49.89	50.53	49.48
Al_2O_3	0.37	<0.01	0.14	<0.01	0.06	<0.01	0.23	<0.01	0.41	0.76	0.15	<0.01
FeO[5]	6.39	5.83	15.37	9.93	2.21	7.13	14.46	10.43	16.77	12.90	15.17	13.41
MgO	6.99	8.71	4.29	6.95	1.49	6.72	6.12	8.99	4.69	5.41	4.44	3.07
MnO	12.59	9.70	8.01	8.34	26.68	11.96	6.03	5.60	7.77	8.77	9.70	11.01
CaO	23.04	23.69	23.33	23.84	22.56	22.41	24.05	23.29	22.35	24.44	21.84	25.00
Total	100.09	99.60	100.72	100.50	102.45	99.08	100.75	99.83	100.14	102.17	101.83	101.97
					Cations based on 6 oxygens							
Si	1.985	2.003	1.976	2.002	1.980	2.014	1.965	1.996	1.945	1.949	1.991	1.960
Al	0.017	0.0	0.007	0.0	0.003	0.0	0.011	0.0	0.195	0.350	0.007	0.0
Fe	0.209	0.189	0.512	0.323	0.074	0.223	0.477	0.338	0.566	0.421	0.500	0.444
Mn	0.417	0.318	0.270	0.275	0.905	0.401	0.201	0.184	0.266	0.290	0.324	0.369
Mg	0.408	0.503	0.255	0.403	0.089	0.397	0.36	0.519	0.282	0.315	0.261	0.181
Ca	0.966	0.984	0.996	0.994	0.968	0.951	1.016	0.967	0.967	1.023	0.922	1.065
Total	4.002	3.997	4.016	3.997	4.019	3.986	4.030	4.004	4.221	4.348	4.005	4.019
Mole percent												
Diopside	39.4	49.8	24.6	40.3	8.3	38.4	34.7	49.9	25.3	30.7	24.1	18.2
Hedenbergite	20.2	18.7	49.4	32.3	6.9	22.8	45.9	32.5	50.8	41.4	46.1	44.6
Johannsenite	40.3	31.5	26.1	27.5	84.7	38.8	19.4	17.7	23.8	28.3	29.8	37.1

Sample no.	1902-48a	929-25a	1431-25a	1902-49a	851-45c	1638-7a	1638-21	1448-81a	1058-103	1638-13	1638-28b
Section no.[1]	21.7	32.9	29.9	21.7	30.3	42.4	50.1	43.5	43.1	44	54.4
Skarn position[2]	S	S	M	M	M	D	D	S	S	M	M
Elevation[3]	M	H	H	M	H	H	H	H	H	H	H
Protolith[4]	C	H	H	C	H	H	C	H	C	H	C
SiO_2	49.93	47.16	48.92	48.92	48.27	53.37	53.15	48.71	48.97	50.44	50.09
Al_2O_3	<0.01	0.15	0.21	0.41	0.15	0.09	0.82	0.40	0.09	<0.01	0.25
FeO	15.85	13.62	7.94	10.62	4.50	9.88	12.27	15.08	13.90	8.04	12.42
MgO	4.39	1.83	2.40	1.98	2.46	9.45	11.08	3.86	6.51	5.06	7.15
MnO	6.21	13.36	19.23	15.01	22.08	5.22	2.86	9.22	6.54	15.06	6.48
CaO	22.94	23.60	22.05	22.99	22.85	22.81	21.62	22.76	24.94	21.22	23.32
Total	99.32	99.72	100.75	99.93	100.31	100.82	101.80	100.03	100.95	99.83	99.71

Cations based on 6 oxygens											
Si	2.004	1.947	1.979	1.987	1.965	2.025	1.992	1.966	1.937	2.009	1.975
Al	0	0.007	0.010	0.020	0.007	0.004	0.036	0.019	0.004	0.0	0.012
Fe	0.532	0.470	0.269	0.361	0.153	0.314	0.385	0.509	0.460	0.268	0.410
Mn	0.211	0.467	0.659	0.516	0.761	0.168	0.091	0.315	0.219	0.508	0.217
Mg	0.263	0.113	0.145	0.120	0.149	0.535	0.619	0.232	0.384	0.300	0.420
Ca	0.986	1.044	0.956	1.000	0.996	0.927	0.869	0.984	1.057	0.906	0.985
Total	3.996	4.048	4.018	4.004	4.031	3.973	3.992	4.025	4.061	3.991	4.019
Mole percent											
Diopside	26.1	10.7	13.5	12.0	14.0	52.6	56.6	22.0	36.1	27.9	40.2
Hedenbergite	52.9	44.8	25.0	36.2	14.4	30.9	35.1	48.2	43.3	24.9	39.1
Johannsenite	21.0	44.5	61.4	51.8	71.6	16.5	8.3	29.8	20.6	47.2	20.7

[1] Section numbers refer to mine sections in Figure 2; Southwest skarn zone = <21, Central skarn zone = 21–41, Northeast skarn zone = >41
[2] Skarn positions: D = dike contact, S = mid-skarn, M = marble front
[3] Elevation: H = high (>4,300 ft), M = medium (4,075–4,300 ft), L = low (<4,075 ft)
[4] Protolith: C = carbonaceous limestone of the Upper, Middle, or Lower Blue limestones, H = pure crinoidal limestone of the Hanover limestone
[5] All iron is FeO

microprobe beam, the individual pyroxenoid analyses appear to span the rhodonite-bustamite miscibility gap described by Albrecht and Peters (1975, 1980). This is probably due to very fine scale intergrowths as described in a transmission electron microscopy (TEM) study by Veblen (1985).

Ilvaite is a relatively rare iron-rich mineral which occurs in some zinc and some calcic iron skarns (Einaudi et al., 1981). In the Groundhog mine ilvaite occurs sporadically as euhedral crystals at the marble front, relict carbonate patches in skarn, and as unaltered crystals in zones of intense chlorite-pyrite retrograde alteration along dike contacts. It is richer in manganese (Table 7) than ilvaite from the zinc skarns at the Pewabic mine, New Mexico (Schmitt, 1939) and South Mountain, Idaho (Sorenson, 1927), but there are too few published ilvaite analyses in the literature for a systematic review.

Compared to most skarn systems, skarn in the Groundhog mine is fresh with relatively little retrograde alteration. Replacement of pyroxene by amphibole is most common in the northeast part of the system, although small amounts of amphibole occur throughout the skarn system. Some of the amphibole is normal actinolite ($Ca_2(Mg,Fe^{+2})_5Si_8O_{22}(OH)_2$), which can be found in most copper skarns (Einaudi, 1982) and the deeper zinc skarns (Einaudi et al., 1981). However, much of the amphibole in the Groundhog mine is subcalcic in nature (Table 8). There appears to be a continuous gradation from full occupancy of the calcium site to about 50 percent occupancy. The subcalcic amphibole is almost always partly to completely replaced by carbonate. In addition, most of the amphiboles are manganese rich (dannemorite) and the manganese content of the amphibole appears to be proportional to that of nearby pyroxene (and presumably that of the replaced pyroxene). The manganese content of amphibole, like that of pyroxene, increases to the southwest.

Fluid Inclusion Study

Fluid inclusion phase changes during heating and freezing studies were measured on a dual purpose heating-freezing stage in the mineral deposit laboratories at Washington State University. The design of the FLUID INC-adapted U. S. Geological Survey gas-flow heating-freezing stage is given in Werre et al. (1979) and sample preparation procedures are described in Meinert (1984). The stage is calibrated periodically using synthetic fluid inclusions available from SYN FLINC (University Park, Pennsylvania) and described by Sterner and Bodnar (1984). Stage accuracy at 374°, 0.0°, and −56.6°C is ± 1.2°, 0.1°, and 0.4°C, respectively.

Detailed sketch maps of each sample were prepared so that specific fluid inclusions could be located and then relocated for subsequent studies. For ho-

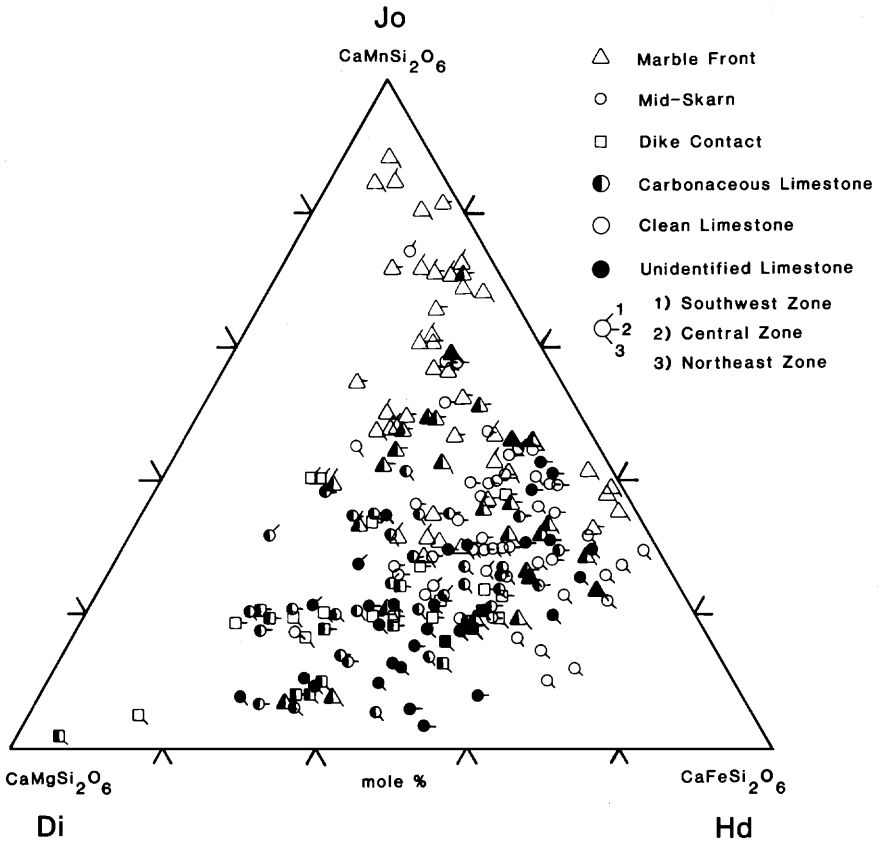

FIG. 6. Triangular plot of diopside (Di), hedenbergite (Hd), and johannsenite (Jo) molecular proportions in pyroxenes from the Groundhog mine, based on electron microprobe analyses. Symbol shape indicates position in skarn. Unfilled shapes = pyroxene formed from coarse-grained, carbonaceous limestone; half-filled shapes = fine-grained impure limestone; filled shapes = protolith composition not identified with certainty; tick marks = sample location within the mine.

mogenization studies, a cycling technique (Roedder, 1984) was used in which samples were heated in increments while all inclusions were checked for progress toward homogenization. This technique allows all inclusions in a sample to be heated in one run without overheating individual inclusions. To minimize the possibility of stretching (Bodnar and Bethke, 1984), freezing studies were conducted only after the heating studies were completed.

Suitable fluid inclusions are present in several skarn minerals including garnet, pyroxene, sphalerite, and quartz. More than 500 fluid inclusions, the majority in pyroxene, were analyzed in samples along the length of the skarn system and from the dike contact to the marble front. Most garnets and pyroxenes contain fluid inclusions (5–50 μm), but they are seldom abundant. Most fluid inclusions in garnet occur along growth zones and are assumed to have formed during the growth of the garnet. A typical occurrence of fluid inclusions in pyroxene is a single isolated fluid inclusion or an isolated cluster of fluid inclusions within a single crystal; planar arrays of secondary inclusions are rare to absent. Most fluid inclusions within a grain or adjacent grains of pyroxene have similar homogenization temperatures and are presumed to be of primary origin. In contrast, most quartz and sphalerite grains contain numerous fluid inclusions with many through-going planar arrays of secondary inclusions. In these minerals only fluid inclusions which met Roedder's (1984) textural criteria for primary origin were selected for analysis.

Most analyzed fluid inclusions were two-phase inclusions which homogenized to the liquid phase. A few inclusions were vapor rich and homogenized to a vapor. No immiscible phases, such as liquid CO_2, were observed nor did crushing tests on garnet, pyroxene, and sphalerite in immersion oil indicate the presence of any noncondensable gases in the inclusions. Some garnet and pyroxene crystals from the Northeast skarn zone contain visible daughter minerals tentatively identified as halite and sylvite based on optical properties. Additionally, some pyroxene and sphalerite from the Northeast skarn zone and two occurrences of sphalerite from the Central skarn zone

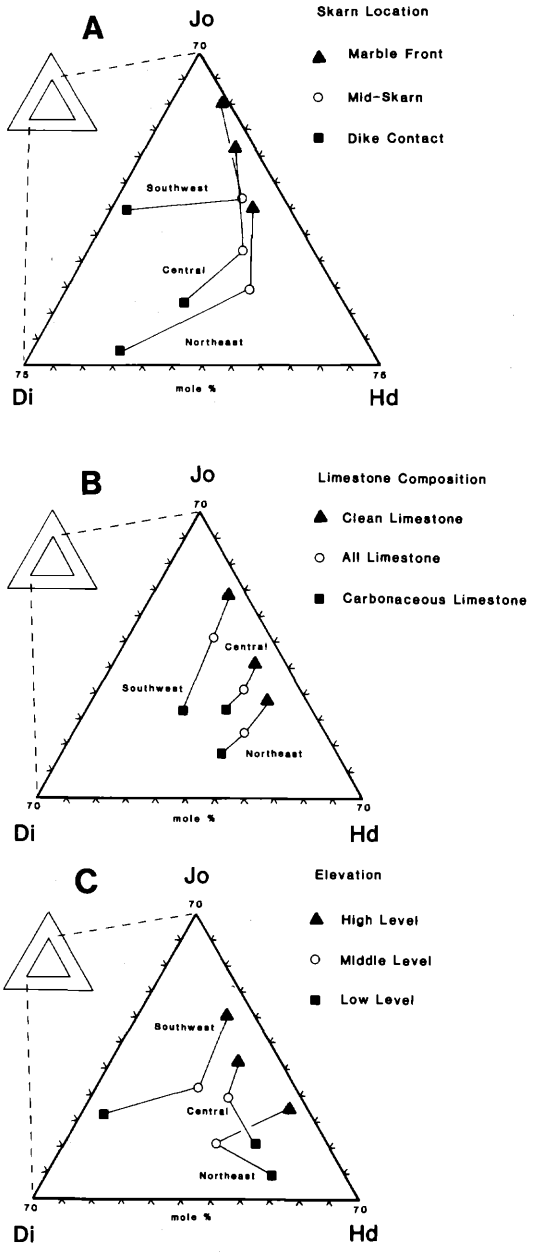

FIG. 7. Average Groundhog pyroxene compositions classified by location in the mine and (A) position within skarn, (B) limestone composition, and (C) elevation.

contain an acicular daughter mineral which did not change upon heating and which might be anhydrite or an iron chloride phase.

Homogenization temperatures of all primary inclusions span a range from 230° to 415°C, but there are systematic differences related to skarn location, skarn position, and mineralogy (Fig. 9). In the Northeast skarn zone, homogenization temperatures of fluid inclusions range from about 300° to 415°C. Fluid inclusion temperatures greater than 350°C are confined to garnet, pyroxene, and sphalerite close to the dike contact and in the mid-skarn region. In contrast, fluid inclusions in pyroxene and sphalerite from close to the marble contact are restricted to temperatures less than 350°C. Homogenization temperatures from sphalerite and quartz in carbonate replacement bodies beyond the limit of skarn in this region span a range similar to pyroxene from skarn at the marble front; however, the average carbonate replacement temperature is slightly lower.

Similar groupings of fluid inclusion homogenization temperatures from the Central and Southwest skarn zones exhibit identical trends. The highest temperatures occur in skarn at the dike contact and the lowest temperatures occur at the marble front and in carbonate replacements beyond the skarn. Moreover, for a given skarn position, the homogenization temperatures are highest in the Northeast zone and lowest in the Southwest zone.

In a further attempt to assess thermal gradients within the Groundhog skarn system, all the fluid inclusion homogenization temperature data have been plotted as a function of distance relative to skarn position (Fig. 10). The best-fit line to the average homogenization temperatures gives an indication of the thermal gradients for a given position within the skarn. The calculated gradients range from a relatively flat 8°C/km close to the dike contact to 23°C/km for skarn formed at the marble front. If the igneous mass of the dike acted as a thermal reserve during infiltration of skarn-forming fluids then it might be expected that thermal gradients would be minimal near the dike and larger away from the dike near the skarn fringe. A comparison of the four calculated gradients (Fig. 11) shows that temperature differences between different parts of the Northeast skarn zone are small, possibly indicating that the thermal flux of dikes and fluids was sufficient to extend beyond the zone of alteration. However, in the southwest part of the system the difference between average temperatures at dike contacts and the limit of alteration is about 50°C, indicating that the skarn-forming fluids were not able to buffer the wall-rock temperature. These temperature ranges and calculated gradients are similar, but due to differences in pluton size and geometry, they are not strictly comparable to those predicted by Johnson and Norton's (1985) theoretical analysis of porphyry-related skarns.

The rare presence of halite and sylvite daughter minerals in garnet and pyroxene fluid inclusions in the Northeast skarn zone indicates that the salinity of the fluid locally exceeded 26 equiv wt percent NaCl. However, these inclusions were too small to measure homogenization of the daughter phases for an accurate salinity determination. For fluid inclusions which do not contain daughter minerals, the salinity can be calculated from the last melting temperature

TABLE 5. Electron Microprobe Analyses of Garnet (in wt %)

Sample no.	1638-27c	1638-27r	1638-15	1642-14	1654-39	1642-16	1642-24
Section no.[1]	54.4	54.4	44	53.4	54.8	53.4	50.7
Skarn position[2]	D	D	D	S	S	M	M
Protolith[3]	C	C	H	H	C	C	H
SiO_2	35.21	35.23	35.49	35.50	35.62	35.56	37.52
Al_2O_3	0.32	0.89	<0.01	0.02	<0.01	0.02	13.11
Fe_2O_3[4]	31.45	30.86	31.63	31.74	31.54	31.21	13.51
MgO	0.02	<0.01	<0.01	0.02	0.02	0.17	0.56
MnO	0.99	0.98	0.49	1.59	0.71	2.10	0.49
CaO	32.67	32.78	32.77	32.06	32.76	31.80	34.67
Na_2O	0.01	0.04	0.03	<0.01	0.08	<0.01	<0.01
TiO_2	0.25	0.12	0.05	0.05	0.12	0.07	1.00
Total	100.92	100.91	100.46	100.99	100.89	100.93	100.87
			Cations based on 24 oxygens				
Si	5.920	5.912	5.985	5.972	5.984	5.986	5.871
Al	0.064	0.176	0.0	0.004	0	0.004	2.418
Fe	3.979	3.897	4.014	4.019	3.991	3.953	1.591
Mg	0.004	0.0	0.0	0.004	0.004	0.042	0.132
Mn	0.142	0.139	0.070	0.226	0.101	0.300	0.065
Ca	5.885	5.893	5.921	5.778	5.896	5.735	5.812
Na	0.002	0.008	0.006	0.0	0.016	0.0	0.0
Ti	0.032	0.015	0.006	0.006	0.015	0.008	0.118
Total	16.028	16.040	16.002	16.009	16.007	16.028	16.007
Mole percent							
Grossularite		2.1					58.0
Andradite	96.2	95.2	97.8	91.5	96.8	90.9	35.7
Pyrope	0.1			0.1	0.1	0.7	2.2
Spessartite	1.5	2.4					1.1
Schorlomite	0.8	0.4	0.2	0.2	0.4	0.2	3.0
Calderite	1.3		2.0	6.2	2.8	8.2	

[1] Section numbers refer to mine sections in Figure 2; Southwest skarn zone = <21, Central skarn zone = 21–41, Northeast skarn zone = >41

[2] Skarn positions: D = dike contact, S = mid-skarn, M = marble front

[3] Protolith: C = carbonaceous limestone of the Upper, Middle, or Lower Blue limestones, H = pure crinoidal limestone of the Hanover limestone

[4] All iron as Fe_2O_3

of the fluid, assuming a simple salt solution (Potter et al., 1978). First freezing temperatures ranged from −49° to −32°C, indicating that some inclusions might also contain $MgCl_2$ or $CaCl_2$. Salinities were determined for 51 inclusions from 14 different skarn samples (Fig. 12). In general, fluid inclusions from the Northeast skarn zone are higher temperature and higher salinity (the average for inclusions without daughter minerals is 337°C and 8.5 equiv wt % NaCl) than more distal fluid inclusions. Fluid inclusions from the Central skarn zone are slightly higher in temperature and salinity (avg, 320°C and 7.3% NaCl) than those from the Southwest zone (avg, 293°C and 6.2% NaCl).

Two pyroxene samples from the Northeast zone contain spatially associated, cogenetic groups of fluid inclusions that homogenized either to a vapor phase or to a liquid phase; both sets of fluid inclusions in both samples homogenized at 340°C and are taken as evidence for boiling. A freezing determination on a liquid-rich inclusion in one of the samples yielded a salinity of 6.3 percent NaCl, whereas inclusions from the other sample yielded a salinity of 9.5 percent NaCl. Using the data of Sourirajan and Kennedy (1962), the trapping pressure determined from these two samples is 175 and 155 bars, respectively. These pressures correspond to depths of 660 to 585 m assuming purely lithostatic conditions and 1,785 to 1,580 m assuming purely hydrostatic conditions. Although the absolute depth of these samples at the time of mineralization is unknown, they were collected from a depth in the mine 600 m beneath the present land surface. Thus, conditions at the time of boiling were probably closer to hydrostatic than

TABLE 6. Electron Microprobe Analyses of Pyroxenoid (in wt %)

Sample no.	1166-99b	1654-35b	1902-102b	1902-116a	1902-71	900-13a
Section no.[1]	14.6	56.3	7.2	−2.5	19.5	47.3
Skarn position[2]	S	S	M	M	M	M
Protolith[3]	C	C	H	H	H	H
SiO_2	48.09	46.85	48.05	47.55	47.32	46.88
Al_2O_3	<0.01	0.13	0.02	<0.01	<0.01	0.13
FeO[4]	6.63	7.72	4.67	6.37	3.82	2.89
MgO	2.45	1.19	0.27	0.80	0.66	0.15
MnO	34.51	38.72	34.19	36.66	42.25	39.41
CaO	8.56	5.51	13.76	8.20	6.50	10.49
Total	100.25	100.12	100.96	99.59	100.56	99.95
			Cations based on 18 oxygens			
Si	6.020	5.893	6.000	6.051	6.017	5.974
Al	0.0	0.020	0.003	0.0	0.0	0.020
Fe	0.694	0.824	0.488	0.678	0.406	0.308
Mn	0.458	0.227	0.050	0.151	0.126	0.028
Mg	3.659	4.188	3.616	3.951	4.549	4.254
Ca	1.148	0.754	1.841	1.118	0.885	1.432
Total	11.979	11.906	11.998	11.949	11.983	12.016
Mole percent						
$MnSiO_3$	61.4	69.9	60.3	67.0	76.2	70.6
$CaSiO_3$	19.3	12.6	30.7	19.0	14.8	23.8
$(Fe, Mg)SiO_3$	19.3	17.5	9.0	14.1	8.9	5.6

[1] Section numbers refer to mine sections in Figure 2; Southwest skarn zone = <21, Central skarn zone = 21–41, Northeast skarn zone = >41

[2] Skarn positions: D = dike contact, S = mid-skarn, M = marble front

[3] Protolith: C = carbonaceous limestone of the Upper, Middle, or Lower Blue limestones, H = pure crinoidal limestone of the Hanover limestone

[4] All iron as FeO

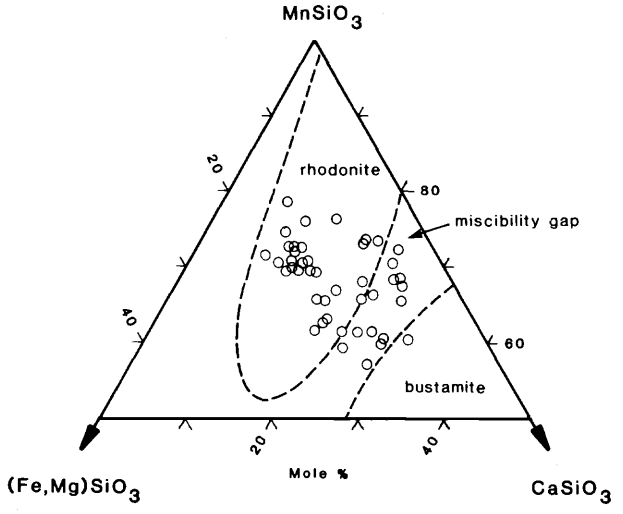

FIG. 8. Triangular plot of ferrosilite (Fe, Mg)SiO_3, wollastonite ($CaSiO_3$), and rhodonite ($MnSiO_3$) molecular proportions in pyroxenoids from the Groundhog mine, based on electron microprobe analyses. Pyroxenoid miscibility gap shown by dashed lines (from Albrecht and Peters, 1980).

lithostatic. However, an increase in pressure of 25 to 50 bars, which could easily occur under more lithostatic conditions, would have been sufficient to prevent boiling of even the hottest fluids documented in the Groundhog skarn system. Thus, the bulk of the skarn in the Groundhog system probably formed under dominantly hydrostatic conditions and boiling occurred on a small scale when the pressure fluctuated from more lithostatic to more hydrostatic conditions.

Summary and Discussion

The Groundhog skarn system is associated spatially with a near-vertical swarm of granodiorite porphyry dikes. It is thus toward the distal manganese-rich end of the zinc skarn hierarchy summarized by Einaudi et al. (1981). Like many of these skarns, the Groundhog skarn is zoned in terms of its metal content and skarn mineralogy. The Groundhog skarn system is exceptional in that it is zoned over a >3-km strike length. The documented gradients in skarn mineralogy, composition, and fluid evolution provide the basis for a

TABLE 7. Electron Microprobe Analyses of Ilvaite (in wt %)

Sample no.	1638-26	1902-13	1902-47	1902-55a
Section no.[1]	54.4	40	21.7	20.1
Skarn position[2]	M	S	S	S
Protolith[3]	C	C	C	H
SiO_2	29.09	28.94	35.64	30.42
Al_2O_3	0.16	0.52	0.09	<0.01
FeO[4]	41.73	42.74	34.86	38.89
MgO	0.04	0.26	1.98	0.58
MnO	11.79	9.19	9.71	11.58
CaO	12.65	13.42	15.43	13.79
K_2O	<0.01	<0.01	<0.01	<0.01
Na_2O	<0.01	<0.01	<0.01	<0.01
TiO_2	<0.01	<0.01	<0.01	<0.01
Total	95.49	95.10	97.74	95.30
Cations based on 8.5 oxygens				
Si	2.114	2.101	2.361	2.176
Al	0.014	0.044	0.007	0
Fe	2.536	2.595	1.931	2.327
Mn	0.004	0.028	0.196	0.062
Mg	0.725	0.565	0.595	0.701
Ca	0.985	1.044	1.095	1.057
Total	6.378	6.377	6.185	6.323

[1] Section numbers refer to mine sections in Figure 2; Southwest skarn zone = <21, Central skarn zone = 21–41, Northeast skarn zone = >41

[2] Skarn positions: D = dike contact, S = mid-skarn, M = marble front

[3] Protolith: C = carbonaceous limestone of the Upper, Middle, or Lower Blue limestones, H = pure crinoidal limestone of the Hanover limestone

[4] All iron as FeO

possible model of zinc skarn formation consistent with the general classification of Einaudi et al. (1981).

Metal zonation

Skarn production together with reserve data well illustrate the systematic base metal zonation within the Groundhog mine. Both Zn/Cu and Pb/Cu ratios increase toward the distal southwest part of the system (Table 1). Additionally, lead grades increase by more than 400 percent from northeast to southwest. In contrast, copper grades are highest in the proximal northeast part of the system, although this is masked somewhat by a change in mineralogical habit. In the Northeast skarn zone, copper occurs mainly as a separate phase in the form of massive chalcopyrite associated with garnet, whereas in the Central and Southwest zones, chalcopyrite occurs only as inclusions within sphalerite. Similar trends have been observed at the Pewabic mine, New Mexico, where Schmitt (1939) noted that copper in the form of chalcopyrite is most concentrated at depth and near the Hanover pluton. At Aguilar, Argentina (Spencer, 1950), and at Ban Ban, Australia (Ashley, 1980), there is a transition from Pb to Zn to Cu with depth, and in the Yeonhwa-Ulchin district, Korea, Yun and Einaudi (1982) reported that Pb/Zn ratios increase upward (presumably more distal) within the skarns. As in the Groundhog mine, the metal zonation in the Yeonhwa I and II mines correlates with a calc-silicate mineralogical transition from garnet to pyroxene to pyroxenoid (Yun and Einaudi, 1982).

Skarn mineralogy

Like many skarns, there is a calc-silicate zonation sequence of garnet-pyroxene-pyroxenoid in the Groundhog mine from dike to marble. There is also a similar zonation from northeast to southwest within the skarn system. Thus it is possible to compare a mineralogical zonation developed on the scale of meters with a similar sequence developed on the scale of kilometers.

Exoskarn in the Northeast zone part of the system is zoned from garnet-pyrite-magnetite-chalcopyrite-sphalerite near the dike contact to pyroxene-sphalerite-pyrite-magnetite-hematite in the mid-skarn region to pyroxene-pyroxenoid-sphalerite-galena ± pyrite-hematite at the marble front. Minor quartz and carbonate occur interstitial to calc-silicate minerals and in patches throughout the skarn. Beyond skarn, the limestone is bleached and locally replaced by mantos or chimneys of sphalerite-pyrite-quartz-carbonate ± chlorite. Similar zonation sequences are found in many skarn deposits, particularly zinc skarns (e.g., Titley, 1961; Bartholomé and Evrard, 1970; Yun, 1979; Dilles, 1981).

In general, this skarn zonation sequence is much wider and more fully developed in the pure coarse-grained Hanover limestone than in the impure fine-grained Blue limestones (a similar relationship was noted for skarn in the Pewabic mine, Schmitt, 1939). This difference can be ascribed to permeability; skarn-forming fluids were able to penetrate farther and with higher water/rock ratios in the coarser grained limestone. Higher X_{CO_2} in the carbonaceous Blue limestones caused by oxidation of carbon may also have had an effect by inhibiting skarn growth.

The overall skarn zonation along the entire strike length is similar to that from dike to marble at specific localities. In the northeast, garnet occurs at the dike contact. In the Central skarn zone, garnet is absent and pyroxene begins the zonation sequence at the dike contact. Farther to the southwest, pyroxene is sparse to absent and pyroxenoid begins the zonation sequence. In addition to this mineralogical zonation along strike, there is a change in relative mineral abundance. For example, although pyroxenoid and galena occur at the marble front in the Northeast zone, there is significantly more pyroxenoid and galena in the Southwest zone.

TABLE 8. Electron Microprobe Analyses of Amphibole (in wt %)

Sample no.	1881-120a	1638-10b	1757-133	1638-7b	1362-141	1479-6
Section no.[1]	57.1	42.4	51.3	42.4	33.2	22.3
Skarn position[2]	S	S	D	D	D	D
Protolith[3]	C	H	H	H	C	H
SiO_2	54.9	53.74	54.1	55.23	53.71	53.31
Al_2O_3	0.52	1.72	0.3	0.34	<0.01	0.3
FeO[4]	11.26	12.68	13.19	14.31	12.94	13.8
MgO	15.29	17.39	14.04	16.8	14.0	12.12
MnO	4.54	3.71	4.79	3.76	4.83	7.66
CaO	9.69	8.02	11.33	6.88	10.93	9.72
K_2O	0.06	<0.01	<0.01	0.06	0.02	<0.01
Na_2O	0.09	0.09	<0.01	0.15	<0.01	<0.01
TiO_2	<0.01	0.10	<0.01	0.08	<0.01	<0.01
Total	96.36	97.46	97.78	97.61	96.46	96.94
			Cations based on 23 oxygens			
Si	7.795	7.738	7.773	7.992	7.802	7.720
Al	0.087	0.292	0.051	0.058	0.0	0.051
Fe	1.336	1.526	1.584	1.731	1.571	1.671
Mn	3.237	3.734	3.008	3.626	3.033	2.618
Mg	0.546	0.453	0.583	0.461	0.595	0.940
Ca	1.474	1.237	1.744	1.067	1.701	1.508
K	0.011	0.0	0.0	0.011	0.004	0.0
Na	0.025	0.025	0.0	0.042	0.0	0.0
Ti	0.0	0.022	0.0	0.009	0.0	0.0
Total	14.511	15.027	14.743	14.997	14.706	14.508
Mole percent						
Mg/(Mg + Fe + Mn)	26.1	26.7	30.6	29.8	30.2	32.0
Fe/(Mg + Fe + Mn)	63.2	65.4	58.1	62.3	58.3	50.1
Mn/(Mg + Fe + Mn)	10.7	7.9	11.3	7.9	11.4	18.0

[1] Section numbers refer to mine sections in Figure 2; Southwest skarn zone = <21, Central skarn zone = 21–41, Northeast skarn zone = >41

[2] Skarn positions: D = dike contact, S = mid-skarn, M = marble front

[3] Protolith: C = carbonaceous limestone of the Upper, Middle, or Lower Blue limestones, H = pure crinoidal limestone of the Hanover limestone

[4] All iron as FeO

Most skarn minerals in the Groundhog mine, including garnet, pyroxene, pyroxenoid, ilvaite, amphibole, chlorite, carbonate, and sphalerite are enriched in manganese. In the case of pyroxene, this manganese enrichment increases toward the marble front (noted by Burt, 1972, for a variety of skarn deposits and by Yun and Einaudi, 1982, for the zinc skarns of the Yeonwha-Ulchin district) and for a given position within skarn, along the entire strike length of the skarn from northeast to southwest. There is also a manganese enrichment at higher elevations and in coarser grained, clean limestones. In each case the more manganese-rich pyroxene can be considered to have formed from fluids which are distal in the overall zonation sequence. In contrast, pyroxene formed in proximal locations (dike contact, Northeast skarn zone, low elevation, fine-grained, impure limestone) is enriched in magnesium. The general sequence of pyroxene-forming fluids, as noted by Burt (1977), is depletion first in Mg, then in Fe, and finally in Mn.

This compositional variation is consistent with available experimental studies of pyroxene stability relations. Gamble's (1982) study of hedenbergite-diopside solid solutions under sulfidizing conditions indicates that addition of 50 mole percent diopside increases the stability of hedenbergite with pyrite relative to andradite by about 100°C. This reaction is also affected by changes in oxygen fugacity because of the presence of Fe^{+2} in hedenbergite and Fe^{+3} in andradite; more oxidizing conditions would favor the formation of andradite and diopsidic pyroxene relative to hedenbergite (Gustafson, 1974; Gamble, 1982). As pointed out by Yun and Einaudi (1982), diopsidic pyroxene could also result from a magnesium-rich fluid due to dolomitic wall rocks.

Manganese is far more effective than magnesium

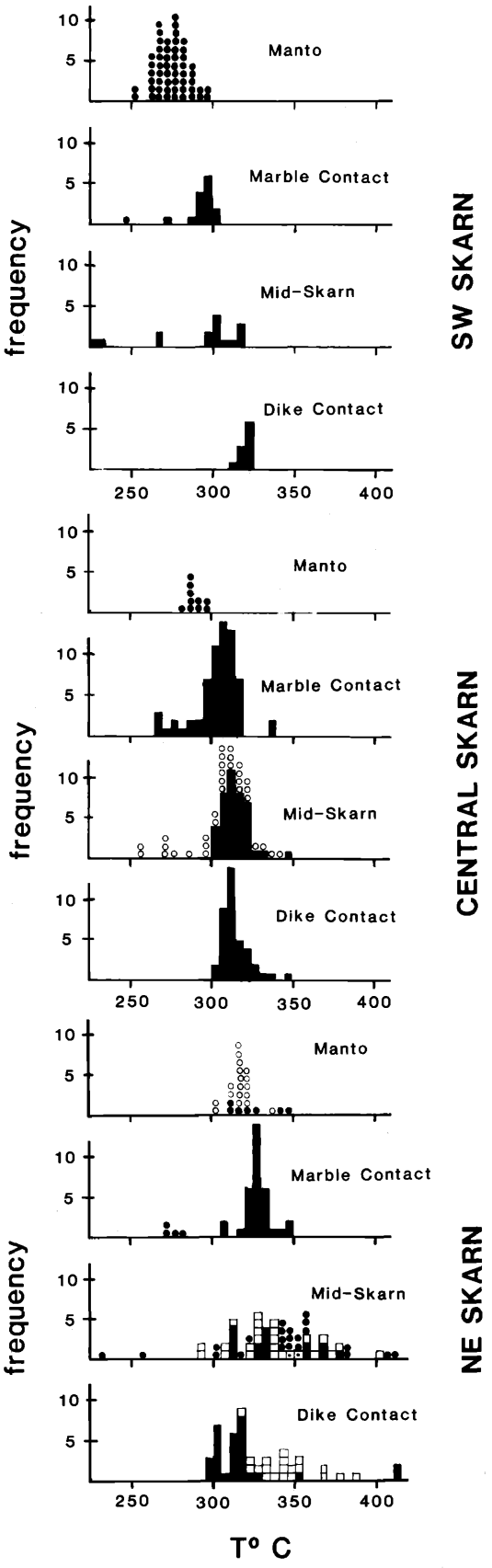

at expanding the clinopyroxene stability field. Burton et al. (1982) have shown that at the 300° to 400°C temperature range of most garnet-pyroxene formation in the Groundhog skarn system, addition of 5 mole percent johannsenite to pure hedenbergite has the same effect in expanding the clinopyroxene stability field as the addition of 40 mole percent diopside. Manganese also affects the low-temperature stability of clinopyroxene (Burton et al., 1982). At 300°C, the addition of 15 mole percent johannsenite to pure hedenbergite increases the stability of clinopyroxene by about 1.5 log f_{S_2} (Fig. 13). Conversely, at a given sulfur fugacity, $Hd_{85}Jo_{15}$ is stable at a temperature about 50°C lower than Hd_{100} (Fig. 13) under the same experimental conditions (Burton et al., 1982).

From the preceding discussion it is apparent that the generalized clinopyroxene enrichment sequence in skarn, Mg-Fe-Mn, could result from a variety of factors including temperature, oxidation state, initial fluid composition, wall-rock composition, and water/rock ratio. Yun and Einaudi (1982) have suggested that distal low Fe/Mn ratios could reflect depletion of the skarn-forming fluid in Fe as iron-rich and manganese-poor garnets were precipitated near proximal channelways. Additionally, Boctor (1985) determined that the Mn/Fe ratio of a fluid in the system MnO-SiO_2-HCl-H_2O increases with an increase in pH, as might be expected of a fluid reacting with carbonate at the marble front. In the absence of more complete experimental data on pyroxene solid solutions, it is not possible to offer a unique explanation for the observed pyroxene compositional variability in the Groundhog skarn system. However, the correlation between the observed trends in pyroxene composition (from dike to marble and from northeast to southwest) and fluid inclusion homogenization temperature-salinity is consistent with a model in which skarn-forming fluids evolve by progressive reaction with carbonate rocks as temperatures decline.

Fluid inclusions

The average and maximum fluid inclusion homogenization temperatures recorded from skarn in the Groundhog mine are lower than temperatures determined for most other zinc skarns (550°–400°C at Zimapan, Mexico, Lindgren and Whitehead, 1914; 490°–390°C at Washington Camp, Arizona, Surles, 1978; 450°–275°C at Nakatatsu, Japan, Shimizu and Iiyama, 1982; 360° ± 28°C at Hanover, New Mexico, Turner and Bowman, 1984). Fluid inclusion homogenization temperatures and salinities apparently are zoned within the Groundhog skarn system. In the

FIG. 9. Histograms of fluid inclusion homogenization temperatures from the Groundhog mine. Open squares = garnet, filled squares = pyroxene, open circles = quartz, and filled circles = sphalerite.

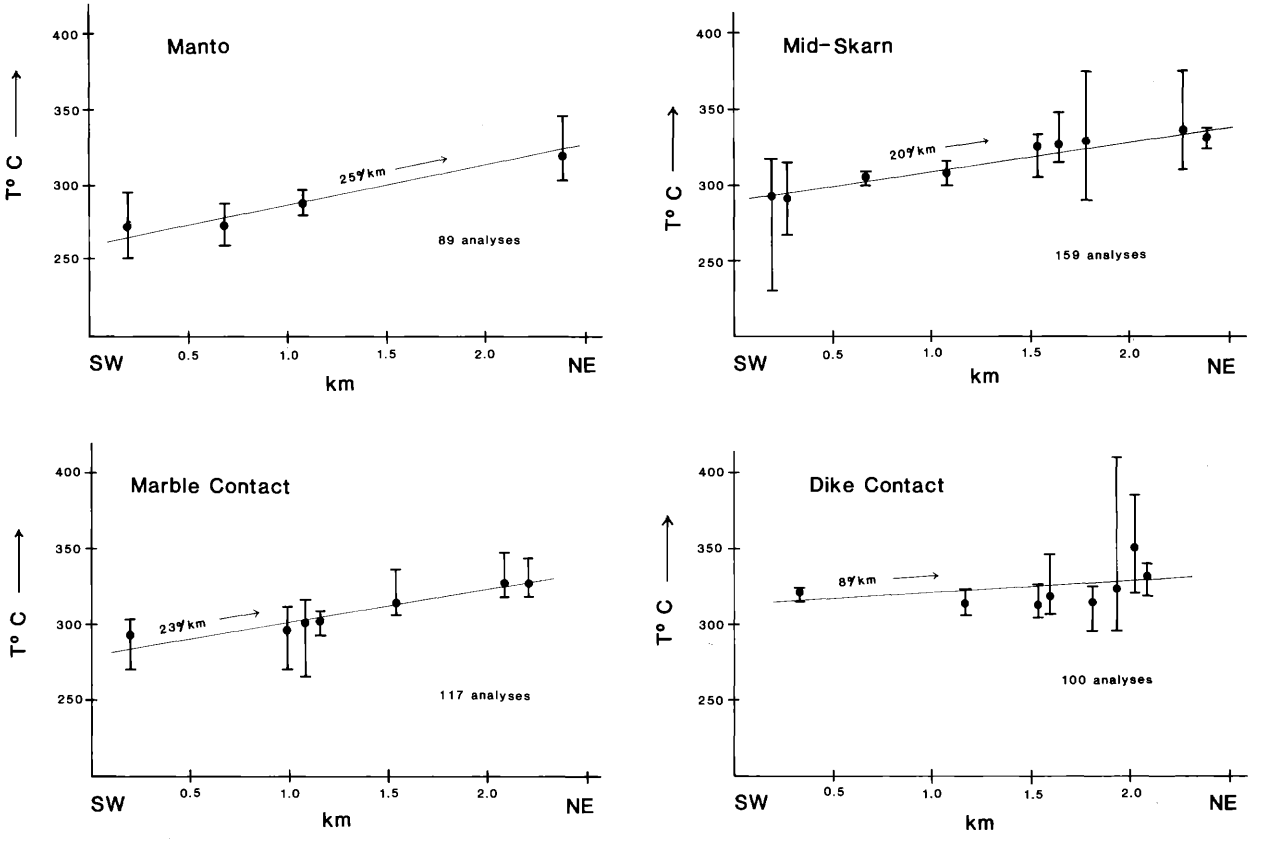

FIG. 10. Fluid inclusion homogenization temperatures from the Groundhog mine plotted as a function of distance along strike of the skarn system. Average and range for each sample shown with thermal gradients calculated from best-fit line to average homogenization temperatures.

Northeast skarn zone the average homogenization temperature is 337°C and the presence of salt daughter minerals indicates that the fluid salinity locally exceeded 26 equiv wt percent NaCl (average salinity for fluid inclusions in this zone which do not contain daughter minerals is 8.5 equiv wt % NaCl). In the Central and Southwest skarn zones salt daughter minerals are absent and average homogenization temperatures and salinities are, respectively: 320°C and 7.3 wt percent NaCl and 293°C and 6.2 wt percent NaCl. Such low skarn temperatures are relatively rare, having only been reported (~300°C) for the Uchucchacua vein deposit in Peru which contains trace amounts of johannsenite and bustamite (Alpers, 1980).

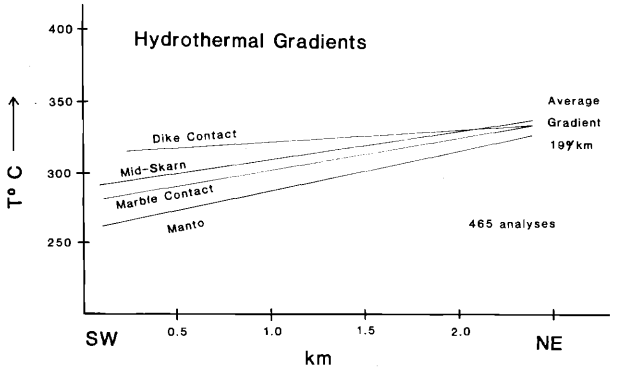

FIG. 11. Superimposed hydrothermal gradients for different skarn positions calculated from fluid inclusion homogenization temperatures of Figure 9.

Temperature gradients calculated from plots of fluid inclusion inclusion homogenization temperatures (Fig. 10) indicate that fluid temperatures decline toward the distal southwest end of the skarn system and from dike to marble. Calculated gradients along strike are small near the dike contact (8°C/km) and become progressively larger toward the marble contact (23°C/km) and in carbonate replacements (25°C/km) beyond the skarn (Fig. 10). For the nearly 3-km strike length of the Groundhog skarn system, these gradients would yield a temperature decline along strike of 25°C at the dike contact and 70°C at the marble contact and an average decline of about 35°C from dike contact to the marble front and 50°C from the dike contact to the limit of alteration (the mantos). Such gradients could be interpreted to result from progressive interaction and dilution of hot, relatively

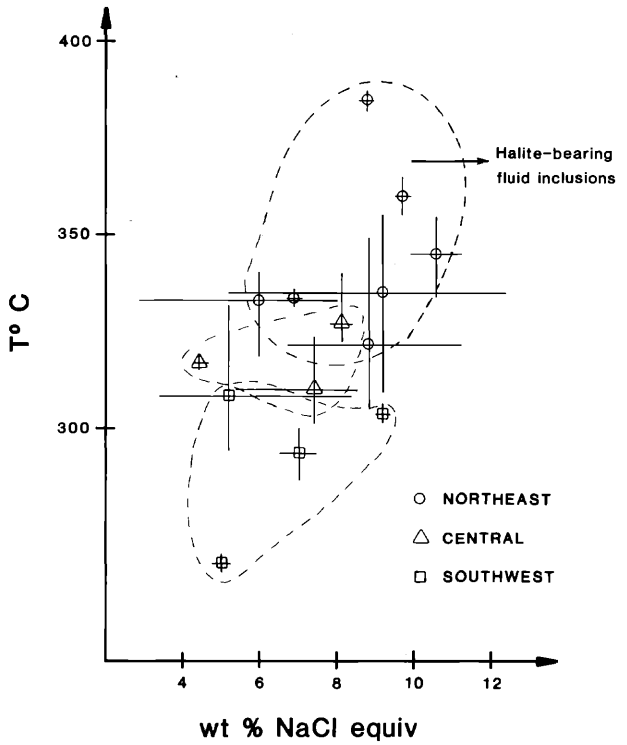

FIG. 12. Plot of fluid inclusion homogenization temperatures and salinity (calculated from freezing point depression using data of Potter et al., 1978) for garnet and pyroxene skarn. Average and range shown for each sample.

saline hydrothermal fluids with cooler, more dilute meteoric water. Convoluted fluid flow paths along faults, stratigraphic contacts, and local modifications by protolith permeability contrasts and varying water/rock ratios would undoubtedly lead to a very complicated final picture. Indeed, the variability of individual skarn samples (Fig. 10) is quite large.

Comparison of the calculated thermal gradients, observed pyroxene compositions, and the limited experimental data on Mg-Fe-Mn pyroxene stability yields some broad areas of agreement. The distal portions of skarn (marble front and Southwest zone) have the most manganese-rich pyroxenes and the lowest fluid inclusion homogenization temperatures. The difference in average johannsenite content between all pyroxenes formed in the Northeast and Southwest skarn zones is 13 mole percent. The measured difference in fluid inclusion homogenization temperatures between these two zones is 44°C, in general agreement with the 50°C difference that 15 mole percent johannsenite made experimentally in the stability of hedenbergite pyroxene (Burton et al., 1982). Similarly, the difference in average johannsenite content between all pyroxenes formed at the dike contact and those formed at the marble front is 19 mole percent. The calculated temperature difference between these two locations is 35°C. It would appear that manganese enrichment is more dramatic, and possibly less a function of temperature, in skarn formation perpendicular to the dike contact than along the 3-km strike length. This in turn probably reflects the contrast between relatively rapid transport along the dike contact with little wall-rock reaction and complete dilution and exhaustion of the fluid during reaction with carbonate rocks. The hierarchy of zinc skarns summarized by Einaudi et al. (1981) possibly represents a similar continuum ranging from proximal fluid reaction with carbonate rocks, to distal transport and fluid evolution prior to complete fluid exhaustion during reaction with carbonate rocks.

The remarkably consistent trends in skarn mineralogy, composition, and fluid inclusion characteristics from the Groundhog mine can be combined into a highly simplified model which illustrates the range of features found in zinc skarns (Fig. 14). It should be emphasized that even though the illustration is necessarily static, skarn formation is a dynamic process and all zones do not grow simultaneously. Further-

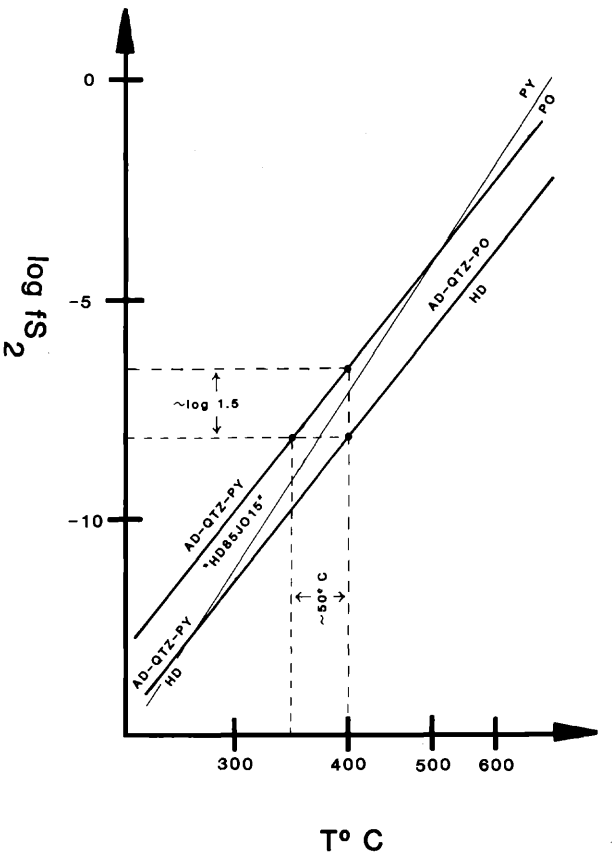

FIG. 13. Log f_{S_2}-T diagram for Hd_{100} and $Hd_{85}Jo_{15}$ sulfidation reactions (after Burton et al., 1982). Ad = andradite, hd = hedenbergite, jo = johannsenite, qtz = quartz, po = pyrrhotite, py = pyrite.

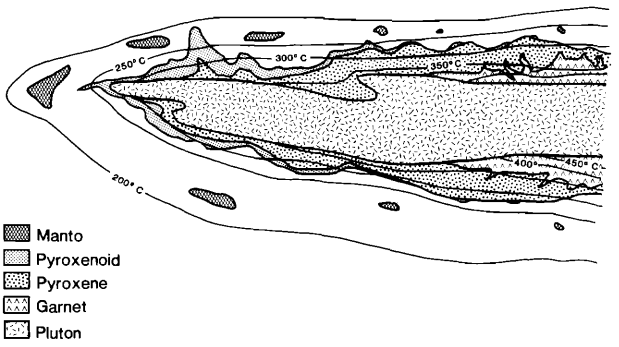

Feature	Distal	Central	Proximal
Gar/pyx	No garnet	1:20	1:1
Max jo in pyx	>50	25–50	<25
Fe oxides	Hm > mt	Hm ~ mt	Mt > hm
Ore sulfides	Sl ~ gl > cp	Sl > gl > cp	Sl > gl ~ cp
Skarn/manto ore	<1	1–10	>10
Temperature	<320°C	320°–400°C	≥400°C
Salinity	<7.5%	7.5–15%	>15%
Zn/Cu (wt %)	>20	10–20	<10
Zn/Pb (wt %)	<2	2–5	>5
Zn/Ag (wt %/oz)	<5	5–10	>10

FIG. 14. Idealized skarn zonation pattern illustrating variations in fluid temperature and composition, skarn mineralogy, and metal ratios from proximal to distal zinc skarns. Based on data from the Groundhog mine and sources cited in text. Cp = chalcopyrite, gar = garnet, gl = galena, hm = hematite, jo = johannsenite, mt = magnetite, pyx = pyroxene.

more, most zinc skarns would represent only a portion of this general model.

Of particular importance is the transition from skarn to the compositionally similar sulfide carbonate replacements beyond skarn. These zones can be quite high grade and are analogous to the very large manto and chimney replacement deposits in Mexico (e.g., Hewitt, 1943, 1968; Ruiz, 1983), which contain few if any calc-silicate minerals, or the large carbonate replacement deposits in western North America (Gemmill, 1968; Morris, 1968; Tweto, 1968; Thompson et al., 1983; Abbott, 1985). Because the carbonate replacements in the Groundhog mine are compositionally similar to skarn, temperature, salinity, and water/rock ratio are possibly the critical variables in their formation.

Conclusions

The Groundhog skarn system is zoned systematically with respect to metal ratios, mineralogy, composition, and fluid inclusion homogenization temperatures. Variations in metal ratios and skarn mineralogy are useful aids in comparing and contrasting different skarn deposits. Detailed mapping of skarn mineral proportions and assemblages can be critical in reconnaissance exploration and in the early stages of prospect evaluation. Compositional variations of individual mineral phases and fluid inclusion suites from the Groundhog mine form the basis of a generalized model for zinc skarn formation. The model should have predictive power when used to evaluate similar data from other deposits or, more importantly, from deposits which are only partly exposed or explored. The correlation between metal ratios, ore grades, mineral compositions, and temperatures makes the model a potentially useful exploration guide.

Average pyroxene compositions and fluid inclusion homogenization temperatures from the Groundhog skarn system are consistent with existing experimental data on clinopyroxene stability relations. The generalized pyroxene enrichment sequence Mg-Fe-Mn is interpreted to result largely from fluid depletion and temperature decline. Most skarn minerals are enriched in manganese and the manganese-rich garnets and amphiboles require relatively rare or even theoretical end-member components. Extrapolation of the proposed skarn model would suggest that even more manganese-rich compositions might be found if fluid travel is extensive prior to reaction with carbonate rocks.

Carbonate replacements beyond skarn appear to have formed from the same hydrothermal fluid as skarn, although perhaps more diluted and at slightly lower temperatures. Such zones are possibly analogous to large, high-grade manto and carbonate replacement deposits which do not contain calc-silicate minerals. As such, they provide a link to a deposit class which has no obvious magmatic connection.

Acknowledgments

This study has been several years in the making and many individuals and organizations have contributed to its completion. Initial plans and encouragement were provided during a whirlwind tour of western skarn deposits with Marco Einaudi and Rainer Newberry (funded by National Science Foundation grant EAR 79-19588 to Einaudi). Sal Anzalone of ASARCO has been helpful throughout the study by providing mine access and lodging. Former Groundhog mine manager Steve Hodgson is especially thanked for enthusiasm above and beyond the call of duty. In addition, many mine geologists over the years provided a solid geologic base upon which this study is based; Harrison Schmitt deserves special mention. Mark Hawksworth proved a dedicated assistant in the fluid inclusion study. Jim Reynolds provided an essential psychological and scientific benchmark when he, with proper scepticism, repeated some of the fluid inclusion measurements. Finally, this study would not have been possible without financial support from the National Science Foundation (grant EAR-8212451) and the Washington Mining and Mineral Resource Research Institute.

October 22, 1985; July 7, 1986

REFERENCES

Abbott, G., 1985, Silver-bearing veins and replacement deposits of the Rancheria district: Whitehorse, Dept. Indian Affairs Northern Devel. Yukon Explor. Geology, Geology Sec., 1983, p. 34–35.

Abramson, B. S., 1981, The mineralizing fluids responsible for skarn and ore formation at the Continental mine, Fierro, New Mexico, in light of REE analyses and fluid inclusion studies: Unpub. M.S. thesis, New Mexico Inst. Mining Tech., 143 p.

Ahmad, S. N., and Rose, A. W., 1980, Fluid inclusions in porphyry and skarn ore at Santa Rita, New Mexico: ECON. GEOL., v. 75, p. 229–250.

Albrecht, J., and Peters, T., 1975, Hydrothermal synthesis of pyroxenoids in the system $MnSiO_3$-$CaSiO_3$ at pf = 2 kb: Contr. Mineralogy Petrology, v. 50, p. 241–246.

—— 1980, The miscibility gap between rhodonite and bustamite along the join $MnSiO_3$-$Ca_{0.60}Mn_{0.40}SiO_3$: Contr. Mineralogy Petrology, v. 74, p. 261–269.

Alpers, C. N., 1980, Mineralogy, paragenesis, and zoning of the Luz vein, Uchucchacua, Peru: Unpub. B.A. thesis, Harvard Univ., 138 p.

Ashley, P. M., 1980, Geology of the Ban Ban zinc deposit, a sulfide-bearing skarn, southeast Queensland, Australia: ECON. GEOL., v. 75, p. 15–29.

Barber, C., 1974, Major and trace element associations in limestones and dolomites: Chem. Geology, v. 14, p. 273–280.

Bartholomé, P., and Evrard, P., 1970, On the genesis of the zoned skarn complex at Temperino, Tuscany: Internat. Union Geol. Sci. [Pub.], ser. A, no. 2, p. 53–57.

Boctor, N. Z., 1985, Rhodonite solubility and thermodynamic properties of aqueous $MnCl_2$ in the system MnO-SiO_2-HCl-H_2O: Geochim. et Cosmochim. Acta., v. 49, p. 565–575.

Bodnar, R. J., and Bethke, P. M., 1984, Systematics of stretching of fluid inclusions. I: Fluorite and sphalerite at 1 atmosphere confining pressure: ECON. GEOL., v. 79, p. 141–161.

Burnham, C. W., 1959, Metallogenic provinces of southwestern United States and northern Mexico: New Mexico Bur. Mines Mineral Resources Bull., v. 65, 76 p.

Burt, D. M., 1972, Mineralogy and geochemistry of Ca-Fe-Si skarn deposits: Unpub. Ph.D. thesis, Harvard Univ., 256 p.

—— 1977, Mineralogy and petrology of skarn deposits: Soc. Italiana Mineralogia Petrologia Rendiconti, v. 33, p. 859–873.

Burton, J. C., Taylor, L. A., and Chou, I-M., 1982, The f_{O_2}-T and f_{S_2}-T stability relations of hedenbergite and hedenbergite-johannsenite solid solutions: ECON. GEOL., v. 77, p. 764–783.

Catlin, S. A., 1981, Mineralogy, zoning, and paragenesis of sulfide ores at the Groundhog mine, Central district, New Mexico: Unpub. M.S. thesis, Univ. Arizona, 52 p.

—— 1984, Mineralogy, zoning, and paragenesis of vein and limestone replacement ores at the Groundhog mine, Central district, New Mexico: Geol. Soc. Arizona Digest, v. 15, p. 219–230.

Dilles, P. A., 1981, Skarn formation and mineralization within the Lower Cretaceous Cantarranas Formation, El Mochito mine, Honduras: Unpub. M.S. thesis, Univ. Alaska, 100 p.

Dunn, P. J., 1979, On the validity of calderite: Am. Mineralogist, v. 17, p. 569–578.

Einaudi, M. T., 1982, Skarns associated with porphyry copper plutons, I. Descriptions of deposits, southwestern U. S., II. General features and origin, *in* Titley, S. R., ed., Advances in geology of the porphyry copper deposits, southwestern U. S.: Tucson, Univ. Arizona Press, p. 185–209.

Einaudi, M. T., and Burt, D. M., 1982, Introduction-terminology, classification, and composition of skarn deposits: ECON. GEOL., v. 77, p. 745–754.

Einaudi, M. T., Meinert, L. D., and Newberry, R. J., 1981, Skarn deposits: ECON. GEOL. 75TH ANNIV. VOL., p. 317–391.

Gamble, R. P., 1982, An experimental study of sulfidation reactions involving andradite and hedenbergite: ECON. GEOL., v. 77, p. 784–797.

Gemmill, P., 1968, The geology of the ore deposits of the Pioche district, Nevada, *in* Ridge, J. D., ed., Ore deposits of the United States, 1933-1967 (Graton-Sales vol.): New York, Am. Inst. Mining Metall. Petroleum Engineers, v. 2, p. 1128–1147.

Graf, D. L., and Kerr, P. F., 1950, Trace element studies, Santa Rita, New Mexico: Geol. Soc. America Bull., v. 61, p. 1023–1052.

Graton, L. C., 1910, Georgetown district: U. S. Geol. Survey Prof. Paper 68, p. 318–319.

Gustafson, W. I., 1974, The stability of andradite, hedenbergite, and related minerals in the system Ca-Fe-Si-O-H: Jour. Petrology, v. 15, p. 455–496.

Hernon, R. M., and Jones, W. R., 1968, Ore deposits of the Central mining district, New Mexico, *in* Ridge, J. D., ed., Ore deposits of the U. S., 1933-1967 (Graton-Sales vol.): New York, Am. Inst. Mining Metall. Petroleum Engineers, v. 2, p. 1211–1238.

Hernon, R. M., Jones, W. R., and Moore, S. L., 1964, Geology of the Santa Rita quadrangle, New Mexico: U. S. Geol. Survey Geol. Quad. Map GQ-306, 1:24,000.

Hewitt, W. P., 1943, Geology and mineralization of the San Antonio mine: Santa Eulalia district, Chihuahua, Mexico: Geol. Soc. America Bull., v. 64, p. 173–204.

—— 1968, Geology and mineralization of the main mineral zone of the Santa Eulalia district, Chihuahua, Mexico: Soc. Mining Engineers AIME Trans., v. 241, p. 228–260.

Johnson, J. W., and Norton, D., 1985, Theoretical prediction of hydrothermal conditions and chemical equilibria during skarn formation in porphyry copper systems: ECON. GEOL., v. 80, p. 1797–1823.

Jones, W. R., Hernon, R. M., and Moore, S. L., 1967, General geology of Santa Rita quadrangle, Grant County, New Mexico: U. S. Geol. Survey Prof. Paper 555, 144 p.

Lasky, S. G., 1936, Geology and ore deposits of the Bayard area, Central mining district, New Mexico: U. S. Geol. Survey Bull. 870, 144 p.

—— 1942, Ground Hog mine, Central district, New Mexico, *in* Newhouse, W. H., ed., Ore deposits as related to structural features: Princeton, Princeton Univ. Press, p. 244.

Lasky, S. G., and Hoagland, A. D., 1950, Central mining district, New Mexico: Internat. Geol. Cong., 18th, London, 1948, Rept., Pt. 7, p. 97–110.

Lindgren, W., and Whitehead, W. L., 1914, A deposit of jamesonite near Zimapan, Mexico: ECON. GEOL., v. 9, p. 435–462.

Lindgren, W., Graton, L. C., and Gordon, C. H., 1910, The ore deposits of New Mexico: U. S. Geol. Survey Prof. Paper 68, 361 p.

Lovering, T. G., 1953, Geology of the western portion of the Santa Rita quadrangle, New Mexico: Unpub. M.S. thesis, Univ. Arizona, 44 p.

McDowell, F. W., 1971, K-Ar ages of igneous rocks from the western United States: Isochron/West, no. 2, p. 1–16.

Meinert, L. D., 1983, Variability of skarn deposits: Guides to exploration, *in* Boardman, S. J., ed., Revolution in the earth sciences—advances in the past half century: Dubuque, Iowa, Kendall/Hunt Pub. Co., p. 301–316.

—— 1984, Mineralogy and petrology of iron skarns in western British Columbia, Canada: ECON. GEOL., v. 79, p. 869–882.

Morris, H. T., 1968, The Main Tintic mining district, Utah, *in* Ridge, J. D., ed., Ore deposits of the United States, 1933-1967 (Graton-Sales vol.): New York, Am. Inst. Mining Metall. Petroleum Engineers, v. 2, p. 1043–1073.

Nielsen, R. L., 1968, Hypogene texture and mineral zoning in a copper-bearing granodiorite porphyry stock, Santa Rita, New Mexico: ECON. GEOL., v. 63, p. 37–50.

Paige, S., 1909, The Hanover iron ore deposits, New Mexico: U. S. Geol. Survey Bull., v. 380, p. 199–214.

Paige, S., 1916, Silver City folio, New Mexico: U. S. Geol. Survey Atlas, Folio 199, 19 p.

Parry, W. T., Ballantyne, J. M., and Jacobs, D. C., 1984, Geochemistry of hydrothermal sericite from Roosevelt Hot Springs

and the Tintic and Santa Rita porphyry copper systems: ECON. GEOL., v. 79, p. 72–86.

Potter, R. W., Clynne, M. A., and Brown, D. L., 1978, Freezing point depression of aqueous sodium chloride solutions: ECON. GEOL., v. 73, p. 284–285.

Raymond, R. W., 1870, Statistics of mines and minerals west of the Rocky Mountains (2nd report): Washington, U. S. Treasury Dept., 805 p.

Reynolds, T. J., and Beane, R. E., 1985, Evolution of hydrothermal fluid characteristics at the Santa Rita, New Mexico, porphyry copper deposit: ECON. GEOL., v. 80, p. 1328–1347.

Roedder, E., 1984, Fluid inclusions: Rev. Mineralogy, v. 12, 644 p.

Rose, A. W., 1970, Origin of trace element distribution patterns in sulfides of the Central and Bingham districts, western USA: Mineralium Deposita, v. 5, p. 157–163.

Ruiz, J., 1983, Geology and geochemistry of fluorite ore deposits and associated rocks in northern Mexico: Unpub. Ph.D. thesis, Univ. Michigan, 202 p.

Schmitt, H. A., 1939, The Pewabic mine, New Mexico: Geol. Soc. America Bull., v. 50, p. 777–818.

Schmitt, H. A., 1954, The origin of the silica of the bedrock hypogene ore deposits: ECON. GEOL., v. 49, p. 877–890.

Shimizu, M., and Iiyama, J. T., 1982, Zinc-lead skarn deposits of the Nakatatsu Mine, central Japan: ECON. GEOL., v. 77, p. 1000–1012.

Sorenson, R. E., 1927, The geology and ore deposits of the South Mountain mining district, Owhyee County, Idaho: Idaho. Bur. Mines Geology Pamph. 22, 47 p.

Sourirajan, S., and Kennedy, G. C., 1962, The system H_2O-NaCl at elevated temperatures and pressures: Am. Jour. Sci., v. 260, p. 115–141.

Spencer, A. C., and Paige, S., 1935, Geology of the Santa Rita mining area, New Mexico: U. S. Geol. Survey Bull. 859, 78 p.

Spencer, F. N., Jr., 1950, The geology of the Aguilar lead-zinc mine, Argentina: ECON. GEOL., v. 45, p. 405–433.

Sterner, S. M., and Bodnar, R. J., 1984, Synthetic fluid inclusions in natural quartz. I. Compositional types synthesized and applications to experimental geochemistry: Geochim. et Cosmochim. Acta, v. 48, p. 2659–2668.

Surles, T. L., 1978, Chemical and thermal variations accompanying formation of garnet skarns near Patagonia, Arizona: Unpub. M.S. thesis, Univ. Arizona, 54 p.

Taylor, R. P., and Fryer, B. J., 1983, Strontium isotope geochemistry of the Santa Rita porphyry copper deposit, New Mexico: ECON. GEOL., v. 78, p. 170–174.

Thompson, T. B., Arehardt, G. B., Johansing, R. J., Osborne, L. W., and Landis, G. P., 1983, Geology and geochemistry of the Leadville district, Colorado, *in* White, W. H., ed., The genesis of Rocky Mountain ore deposits—changes with time and tectonics: Denver Region Explor. Geologists Soc. Symposium, Denver, 1983, Proc., p. 101–115.

Titley, S. R., 1961, Genesis and control of the Linchburg ore body, Socorro County, New Mexico: ECON. GEOL., v. 56, p. 695–722.

Turner, D. R., and Bowman, J. R., 1984, A petrologic and fluid inclusion study of the sphalerite skarns at the Empire and Pewabic mines, Hanover, New Mexico [abs.]: Geol. Soc. America Abstracts with Programs, v. 16, p. 678.

Tweto, O., 1968, Leadville district, Colorado, *in* Ridge, J. D., ed., Ore deposits of the United States, 1933–1967 (Graton-Sales vol.): New York, Am. Inst. Mining Metall. Petroleum Engineers, v. 2, p. 681–705.

Veblen, D. R., 1985, TEM study of a pyroxene-to-pyroxenoid reaction: Am. Mineralogist, v. 9, p. 885–901.

Werre, R. W., Bodner, R. J., Bethke, P. M., and Barton, P. B., Jr., 1979, A novel gas-flow fluid inclusion heating/freezing stage [abs.]: Geol. Soc. America Abstracts with Programs, v. 11, p. 539.

Yun, S., 1979, Geology and skarn ore mineralization of the Yeonhwa-Ulchin zinc-lead mining district, SE Tabgaggsan region, Korea: Unpub. Ph.D. thesis, Stanford Univ., 184 p.

Yun, S., and Einaudi, M. T., 1982, Zinc-lead skarns of the Yeonhwa-Ulchin district, South Korea: ECON. GEOL., v. 77, p. 1013–1032.